Tuning the nature and stability of self-assemblies formed by ester benzene 1,3,5-tricarboxamides: crucial role played by the substituents

Alaric Desmarchelier, Bruno Giordano Alvarenga, Xavier Caumes, Ludovic Dubreucq, Claire Troufflard, Martine Tessier, Nicolas Vanthuyne, Julien Idé, Thomas Maistriaux, David Beljonne, Patrick Brocorens, Roberto Lazzaroni, Matthieu Raynal and Laurent Bouteiller

SUPPORTING INFORMATION

General Procedures.

Preparation of new compounds**:** Synthetic procedures for the preparation of **BTA (*R*)-Cha**, **BTA *tert*-Leu**, **BTA Gly**, **BTA Aib** and **^{Me}BTA Val** are detailed in page S35-S38. All amino acids were purchased from Sigma-Aldrich or Alfa Aesar (99% ee) and used as received. All other reagents were purchased from Sigma-Aldrich, Alfa Aesar or TCI and were used directly. **BTA Nle**,[1] **BTA (*R*)-Nle**,[1] **BTA Met**,[1] **BTA (*R*)-Met**,[1] **BTA Phe**,[1] **BTA Ile**,[2] **BTA (*R*)-Ala**,[2] **BTA (*R*)-Abu**,[2] **BTA Val**,[2] **BTA Leu**,[2] **BTA Phg**,[2] and **BTA C8***[3] were prepared following published procedures. Unless otherwise noted, chromatography-grade solvents were used as received. Dried solvents were obtained from an SPS solvent purification system (IT-Inc) and stored on 4 Å molecular sieves. Triethylamine was dried by distillation over CaH_2 and stored over 4 Å molecular sieves. All inert atmosphere reactions were carried out under an argon atmosphere with standard Schlenk-line techniques. NMR spectra were recorded on a Bruker Avance 300 or on a Bruker Avance 600 spectrometer and calibrated to the residual solvent peak: DMSO-d6 (^{1}H: 2.50 ppm; ^{13}C: 39.52 ppm); acetone-d6 (^{1}H: 2.05 ppm; ^{13}C: 29.84 ppm) and toluene-d8 (^{1}H: 2.09 ppm; ^{13}C: 20.40 ppm). Peaks are reported with their corresponding multiplicity (s: singlet; d: doublet, t: triplet; q: quartet; p: pentuplet; hept: heptuplet; dt: doublet of triplets; td: triplet of doublets) and integration, and respective *J* coupling constants are given in Hertz. Exact mass measurements (HRMS) were obtained on TQ R30-10 HRMS spectrometer by ESI+ ionization and are reported in *m/z* for the major signal. **BTA (*rac*)-Cha** (obtained by starting the synthesis with a 1:1 mixture of 3-cyclohexyl-(*R*)-Alanine hydrate and 3-cyclohexyl-(*S*)-Alanine hydrate) and **BTA (*rac*)-*tert*-Leu** were prepared in the purpose of determining the optical purity of **BTA (*R*)-Cha** and **BTA *tert*-Leu** thanks to chiral stationary phase HPLC (see pages S39-S40 for analytical details).

Preparation of BTA solutions for analyses: the desired BTA was weighed into a ø11.6 mm HPLC vial or a ø20 mm glass vial, the volume of solvent was adjusted to the desired end concentration with an adequate glass microsyringe, and verified by weighing the sample. Vials were sealed with PTFE-coated caps to avoid contamination from leaching plasticizer. All ester BTAs dissolve at rt after a few hours on a shaking table (250 rpm) except **BTA Gly** for which heating to 50°C is required for full dissolution. 20 wt% solutions (Fig. S11) were heated to 50°C in order to get homogeneous viscous solutions or gels. The gels showed no syneresis even after 1 month at rt.

Fourier-Transform Infrared (FT-IR) analyses: FT-IR measurements were performed on a Nicolet iS10 spectrometer. FT-IR spectra of the solids were recorded by transmission after evaporation of a CH_2Cl_2

solution of the sample over KBr pellets or by reflection on a Ge probe (ATR-FTIR). Solution spectra were measured in CaF_2 cells by adjusting the pathlength to the concentration: 0.005 cm (2×10^{-1} M, 10^{-1} M), 0.01 cm (5×10^{-2} M, 2.5×10^{-2} M) and 0.02 cm (1×10^{-2} M, 5×10^{-3} M) and were corrected for air, solvent and cell absorption. For VT FT-IR measurements, the temperature was controlled with a digital temperature controller (West 6100+) from Specac and spectra were recorded between KBr pellets for solids and in a KBr cell (pathlength of 0.2 cm) for 2×10^{-3} M solutions. Full spectra were measured every 10 °C (heating rate: 1°C.min^{-1}). Thermal expansion of the solutions was not corrected.

Circular dichroism (CD) analyses: CD measurements were performed on a Jasco J-1500 spectrometer equipped with a Peltier thermostated cell holder and Xe laser (lamp XBO 150W/4). Data were recorded at 20°C (unless otherwise stated) with the following parameters: 20 nm.min^{-1} sweep rate, 0.05 nm data pitch, 2.0 nm bandwidth, and between 350 and 180 nm. The obtained signals were processed as follows: solvent and cell contributions at the same temperature were subtracted and the signals were smoothed (Savitzky−Golay method). Spectra were corrected for solvent and cell contribution. Kuhn anisotropy factors (g) are dimensionless and expressed as follows: $g=\theta/(32980\times Abs)$, where θ is the measured ellipticity (mdeg) and Abs is the absorbance measured at the same wavelength. For CD measurements in solution, the pathlength of the quartz cell was adapted to the concentration: 0.1 mm dismountable quartz cell (2×10^{-3} M), 1 mm quartz cell (5×10^{-5} M) and 10 mm quartz cell (7×10^{-6} M). Molar CD values are reported in L.mol^{-1}.cm^{-1} and are expressed as follows: $\Delta\varepsilon=\theta/(32980\times l\times c)$ where θ is the measured ellipticity (mdeg), l is the optical path length in cm, and c is the concentration in mol.L^{-1}. For VT-CD experiments, the temperature was controlled with a Peltier thermostated cell holder and the pathlength was adapted to the concentration: 0.5 mm-thick sealed capillary for the 1×10^{-3} M and 2×10^{-3} M solutions and 10mm quartz cell for the 7×10^{-6} M solutions. For the 1×10^{-3} M and 2×10^{-3} M solutions, the ellipticity was followed at 255 nm (heating rate: 1°C.min^{-1}). For the 7×10^{-6} M solutions, the ellipticity was followed at 225 nm and 254 nm and full spectra were recorded each 10°C (heating rate: 1°C.min^{-1}). For CD measurements of solids, a $CHCl_3$ solution (8.85 g.L^{-1}) of the sample was spin coated on a quartz plate using a Laurell WS-650-23 spin coater (3000 rpm). For all samples, LD contribution was negligible (ΔLD < 0.005 dOD) and the shape of the CD signal was independent of the orientation of the quartz slide.

UV-Vis analyses: UV-Vis absorption spectra were extracted from CD on each of the above samples and obtained after correction of the absorption of air, solvent, and cell at the same temperature.

Isothermal titrating calorimetry (ITC) analyses: ITC data were recorded on a Microcal VP-ITC apparatus at the desired temperature, injecting 1.2×10^{-3} M (**BTA Aib**), 2×10^{-3} M or 5×10^{-3} M or 1×10^{-2} M (**BTA Met** and **BTA Phe**) cyclohexane solution of the sample into neat cyclohexane. Injections of 5 µL over 10 seconds were performed every 300 seconds at a stirring rate of 260 rpm.

Small-angle neutron scattering (SANS) analyses: SANS measurements were made at the LLB (Saclay, France) on the PACE instrument, at two distance-wavelength combinations to cover the 4×10^{-3} to 0.24Å^{-1} q-range, where the scattering vector q is defined as usual, assuming elastic scattering, as $q=(4\pi/\lambda)\sin(\theta/2)$, where θ is the angle between incident and scattered beam. Data were corrected for the empty cell signal and the solute and solvent incoherent background. A light water standard was used to normalize the scattered intensities to cm^{-1} units.

High-sensitivity differential scanning calorimetry (DSC) analyses: nano-DSC measurements were performed on a TA Instruments nDSC III system in cyclohexane at the desired concentration, between 15 and 75°C, using 3 full heating/cooling cycles, at 1°C.min^{-1}. The reference cell was filled with cyclohexane and the sample cell (0.3 mL) with the solution. The capillary cells were not capped, and a constant pressure of 5 10^5 Pa was applied.

Viscosimetry: viscosimetry measurements were performed on an Anton Paar AMVn falling-ball microviscosimeter with a Ø 0.16 mm capillary, at 25°C at the various concentrations in cyclohexane, with 3 measurements at an angle of +20° and -20°. Results are reported as an average of those 6 measurements.

Differential scanning calorimetry (DSC) analyses: DSC thermograms were measured for neat samples with a TA instrument Q2000 under nitrogen at a scan rate of 20°C.min^{-1}, using 2 full heating/cooling cycles between -80°C and 200°C (except for **BTA Aib** from -80°C to 250°C).

Polarized Optical Microscopy (POM) analyses: POM measurements were performed on a Leica DM 2500 M polarized light microscope equipped with a camera (transmission mode). Textures were obtained from cooling the sample, spread on a microscope glass slide, from its isotropic state.

Molecular modelling: Dimers of **BTA Nle** were built and modelled with the Materials Studio 6.0 modelling package from Accelrys (now Biovia). As a forcefield, Dreiding[4] was used, with charges on the atoms assigned from the polymer consistent force field (PCFF),[5, 6] and a long-range interaction cutoff set to 14 Å with a spline width of 3 Å. The dielectric constant was distance-dependent. The dimers were first submitted to molecular mechanics (MM) energy minimizations using a conjugate gradient algorithm until a convergence criterion of 0.001 kcal per mol.Å was reached. MD simulations were then performed in the canonical (N,V,T) ensemble. The Nose[7] thermal bath coupling was used to maintain the temperature at 298 K, with a coupling constant of 0.01, and the Verlet velocity algorithm was used to integrate the equations of motion during 1 ns, with a 1-fs time step. The energy, H bonds and CD analyses were performed on the structures generated during the last half of the simulation. For the calculation of the CD spectra, the excitonic model was used. Briefly, a supramolecular Hamiltonian was built on the basis of localized excited states. Those states were obtained from CIS calculations performed on isolated molecules using the ZINDO parameterization implemented in the Gaussian package.[8] To ensure the convergence of the spectra up to 150 nm, 60 excited states have been considered. After diagonalization of this Hamiltonian supramolecular transition dipole and magnetic moments were calculated and used to compute the oscillator and rotatory strengths.

NMR analyses: NMR experiments were recorded on a Bruker Avance III 600 spectrometer (14.1T) equipped with an observe broadband probe with z-axis gradient coil with maximum gradient strength of 55.4 G/cm. All spectra were acquired in 5 mm NMR tubes. Each NMR tube contained 10mM of ester BTAs in cyclohexane-d12 (^{1}H, 1.38 ppm). For **BTA Val** and **^{Me}BTA Val**, DOSY experiments were performed using stimulated echo and longitudinal eddy delay with bipolar gradients and two spoil gradients (ledbpgp2s). The diffusion time was Δ = 0.05 s. The duration of the magnetic field pulse gradients $\delta/2$ was adjusted to 2000 µs for **^{Me}BTA Val** and 1700 µs for **BTA Val**. The delay for gradient recovery was 0.1 ms and the eddy current delay 5 ms. For each DOSY-NMR experiment, a serie of 16 spectra on 32 K data points were collected. The pulse gradients (g) were incremented from 2 to 98% of

the maximum gradient strength in a linear ramp with a total experiment time of 55 min. The temperature was set and controlled at 300 K with an air flow of 270 l/h in order to avoid any temperature fluctuations due to sample heating during the magnetic field pulse gradients. After Fourier transformation and baseline correction, the diffusion dimension was processed with the Topspin 2.1 software. Diffusion coefficients, processed with a line broadening of 1 Hz, were calculated by Gaussian fits with Dynamics Center (Bruker software).

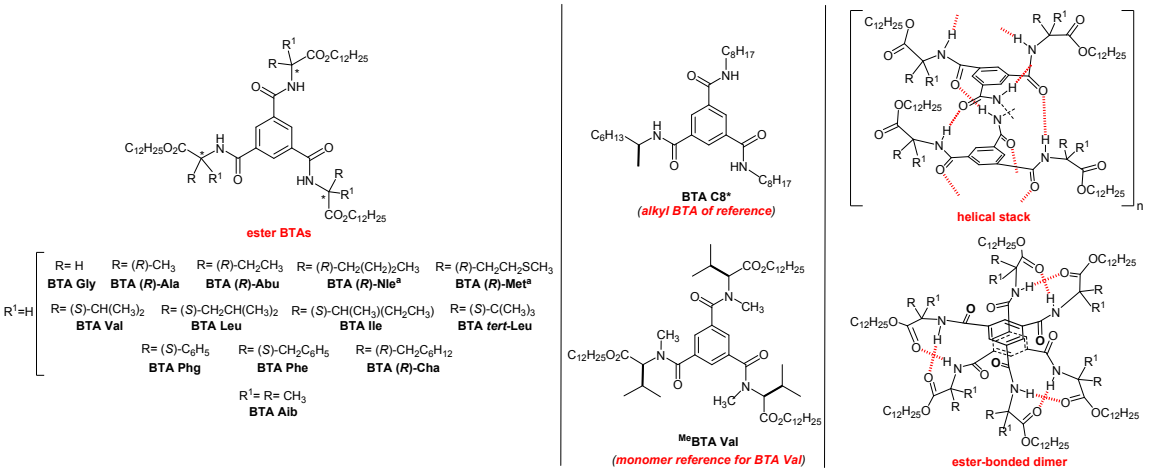

Chemical structures of the BTAs investigated in this study and molecular structures of the rod-like (helical stack) and dimeric hydrogen-bonded species formed by ester BTAs.

Supplementary figures.

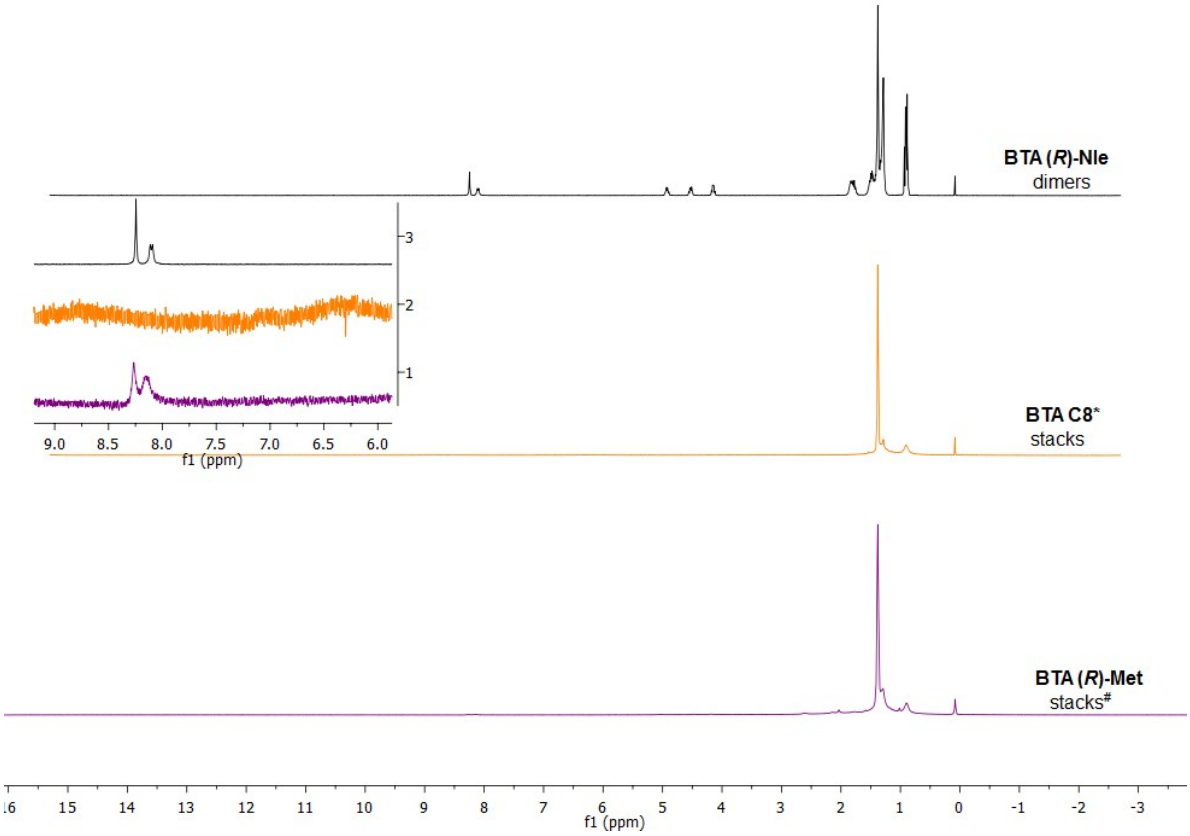

Figure S1. ^{1}H NMR spectra of **BTA (*R*)-Met** (5.1×10^{-3} M), **BTA C8*** (1×10^{-2} M) and **BTA (*R*)-Nle** (1×10^{-2} M) in C_6D_{12} at 20°C. The inset shows a zoom on the region corresponding to the aromatic C-H protons and N-H protons.

[#]At 5.1×10^{-3} M in cyclohexane, **BTA (*R*)-Met** predominantly exists as stacks but *ca.* 11% of dimers are also present as determined by FT-IR analyses (Fig. S21).

a)

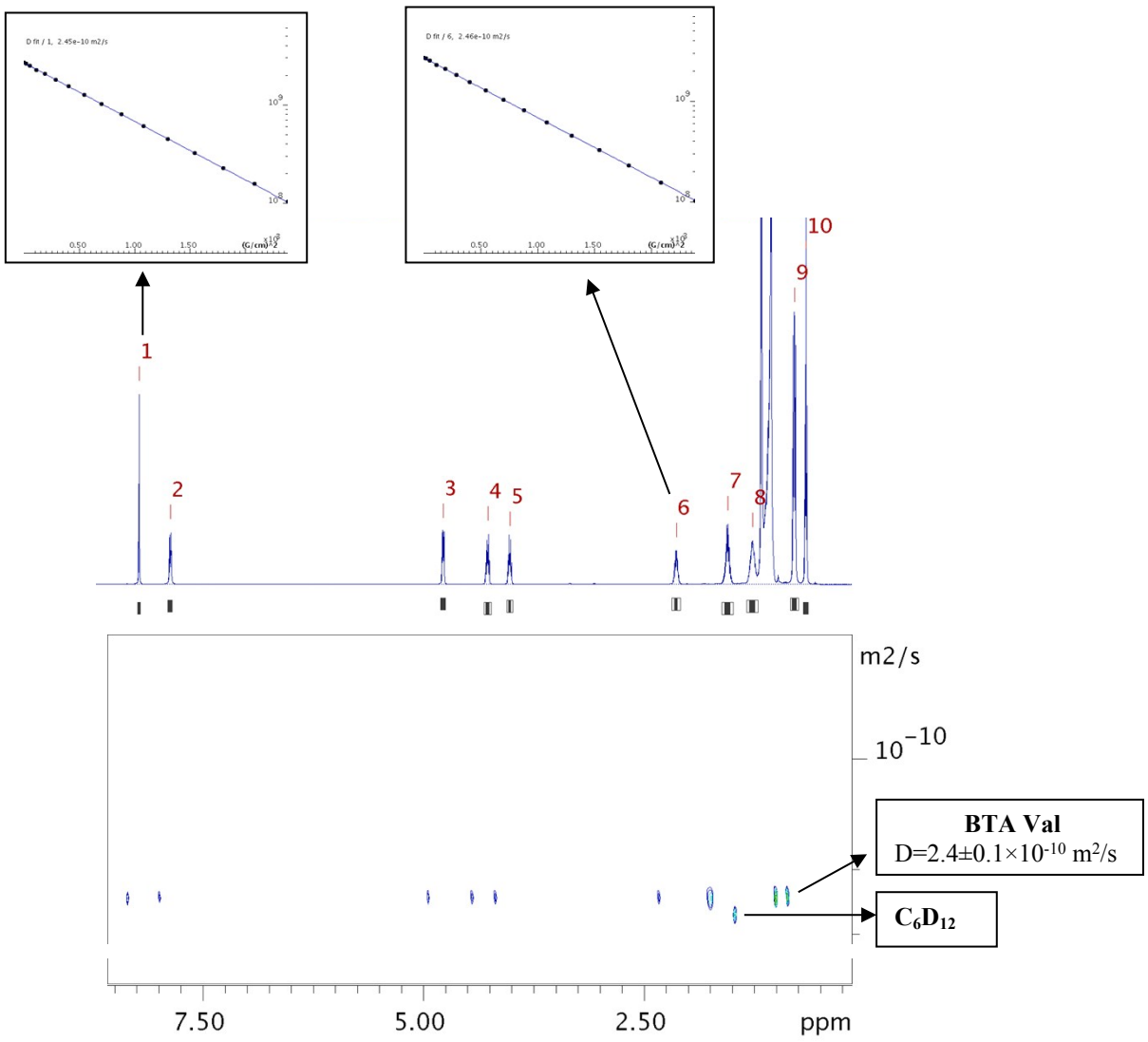
1
2
3
4
5
6
7
8
9
10
m2/s
10^{-10}
BTA Val
D=2.4±0.1×10-10 m2/s
C6D12
7.50
5.00
2.50
ppm

b)

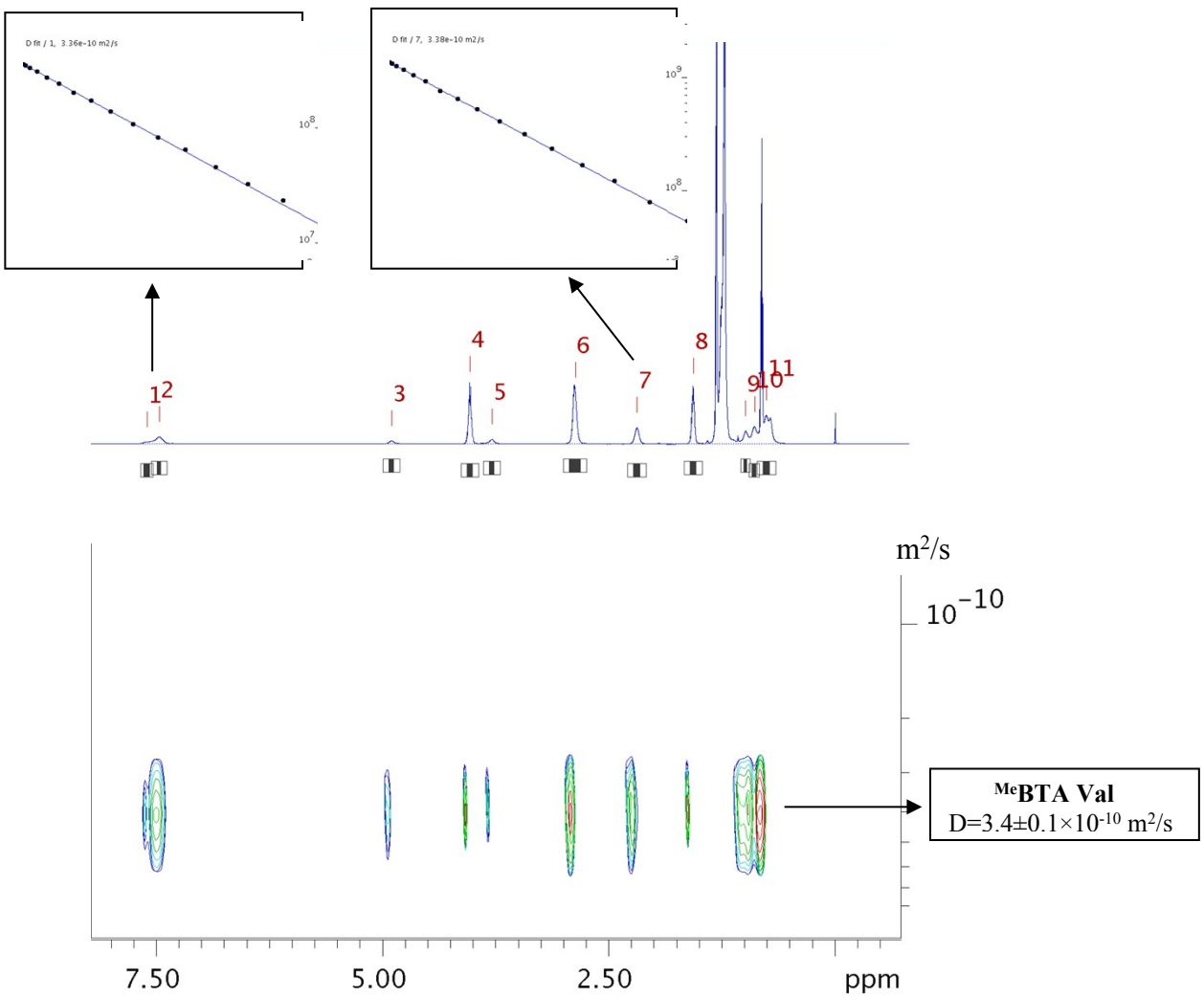

Figure S2. DOSY analyses of **BTA Val** (a) and **^{Me}BTA Val** (b) in C_6D_{12} (10^{-2} M). Indicated diffusion constants are normalized according the value of the diffusion constant found for C_6D_{12} in **BTA Val**. Hydrodynamic radii according to the Stokes-Einstein equation for spherical objects (r_h=(kB×T)/(6×π×η×D)): 10.1±0.1 Å and 7.1±0.1 Å for **BTA Val** and **^{Me}BTA Val** respectively.

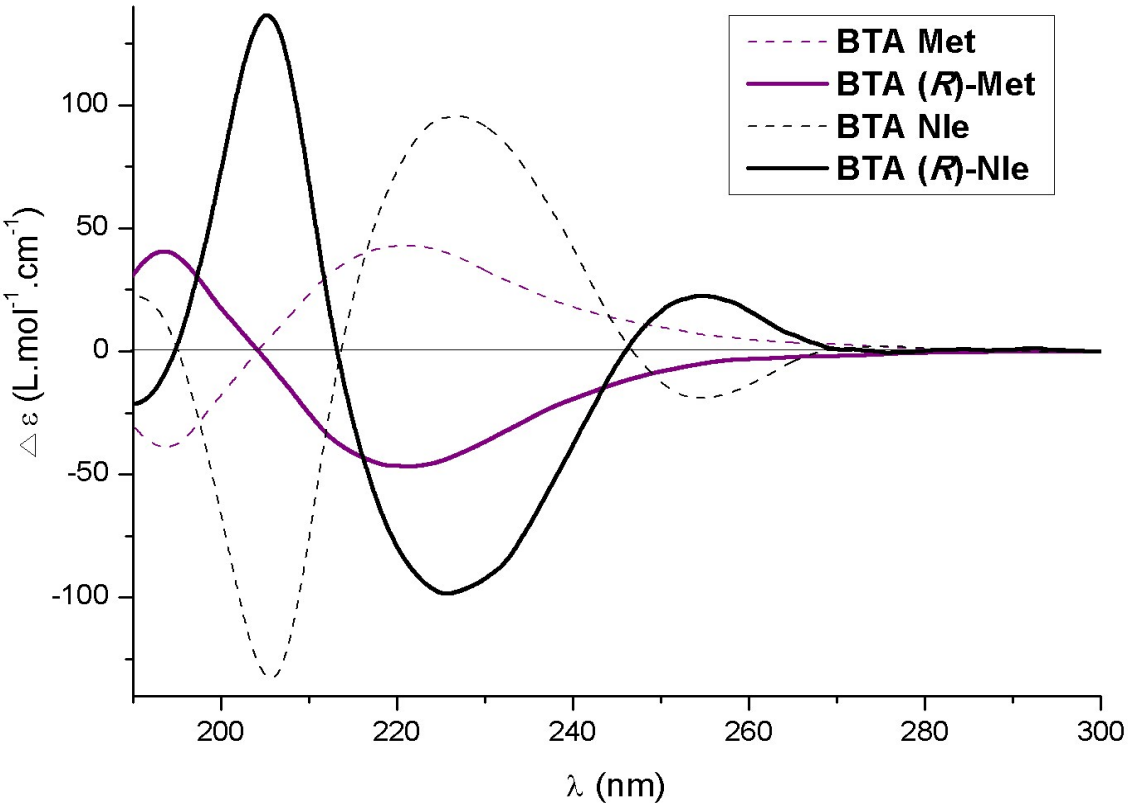

Figure S3. CD spectra of **BTA (*R*)-Met** (2×10^{-3} M) and **BTA (*R*)-Nle** (5×10^{-5} M) and of their enantiomers **BTA Met** (2×10^{-3} M) and **BTA Nle** (5×10^{-5} M) in cyclohexane.

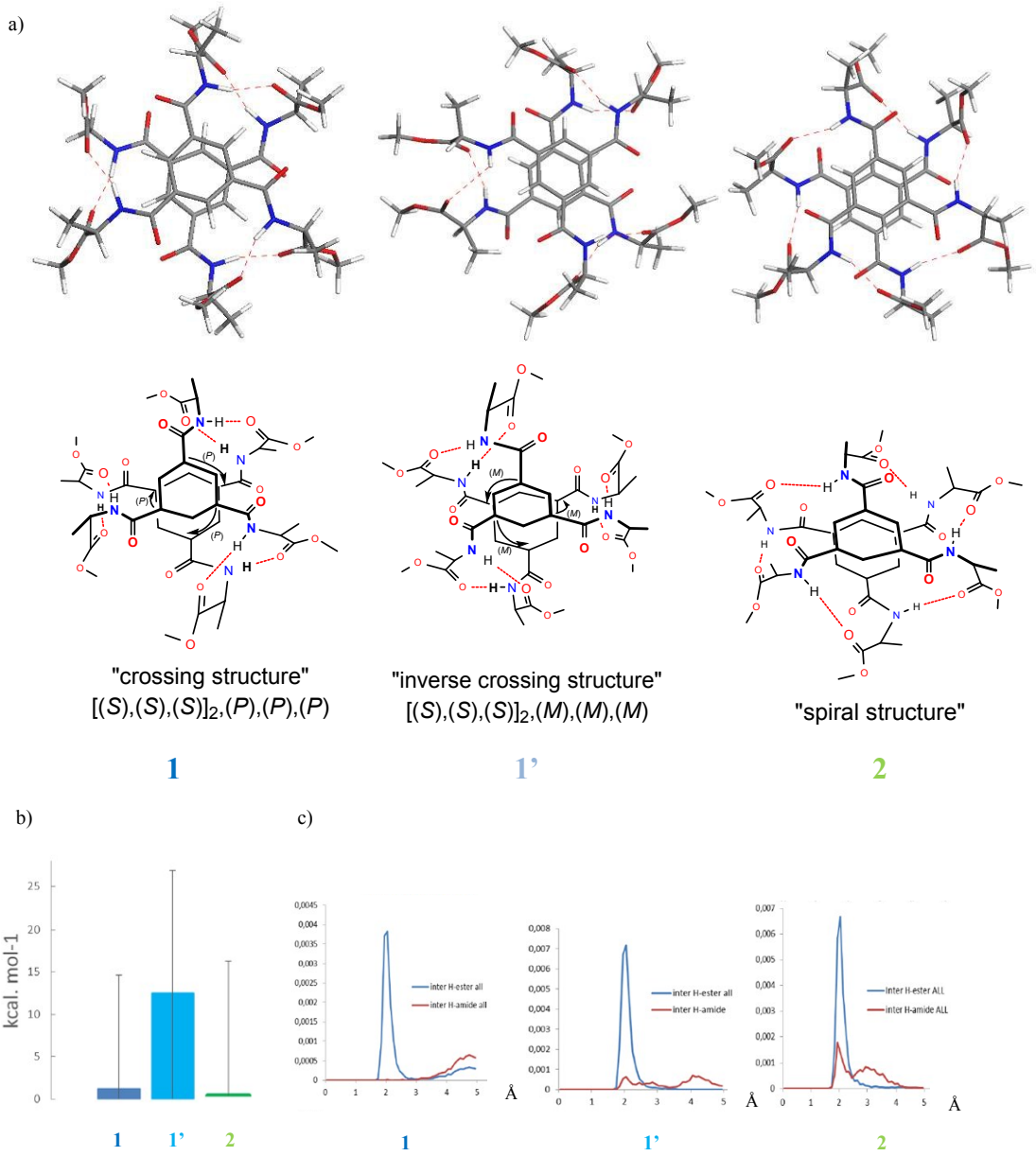

Figure S4. Energy-minimized structures of the "crossing structure" (**1**), the "inverse crossing structure" (**1'**) and the "spiral structure" (**2**) of **BTA Nle** (a). For the sake of clarity, the butyl groups attached to the α-carbons and the dodecyl groups of the ester side chains were replaced by methyl groups. Relative potential energy of the structures (average from the dynamics) (b). Radial distribution function between the amide hydrogens and the ester (and amide) oxygens of the structures (average from the dynamics). The peak at 2 Å corresponds to hydrogen bonds (c).

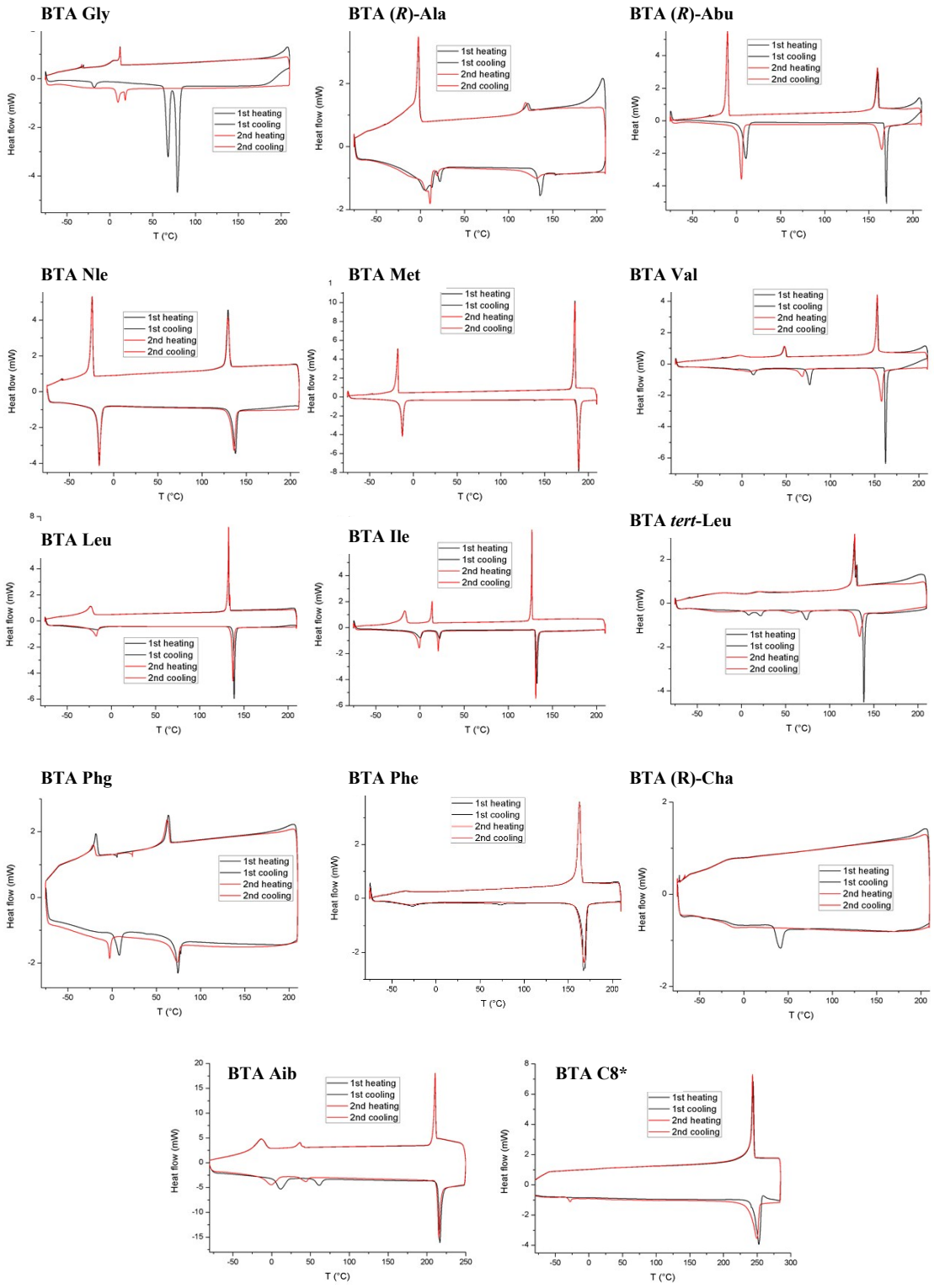

Figure S5. DSC traces of ester BTAs and of **BTA C8*** in the bulk (20°C.min^{-1}). Endothermal peaks are directed downward.

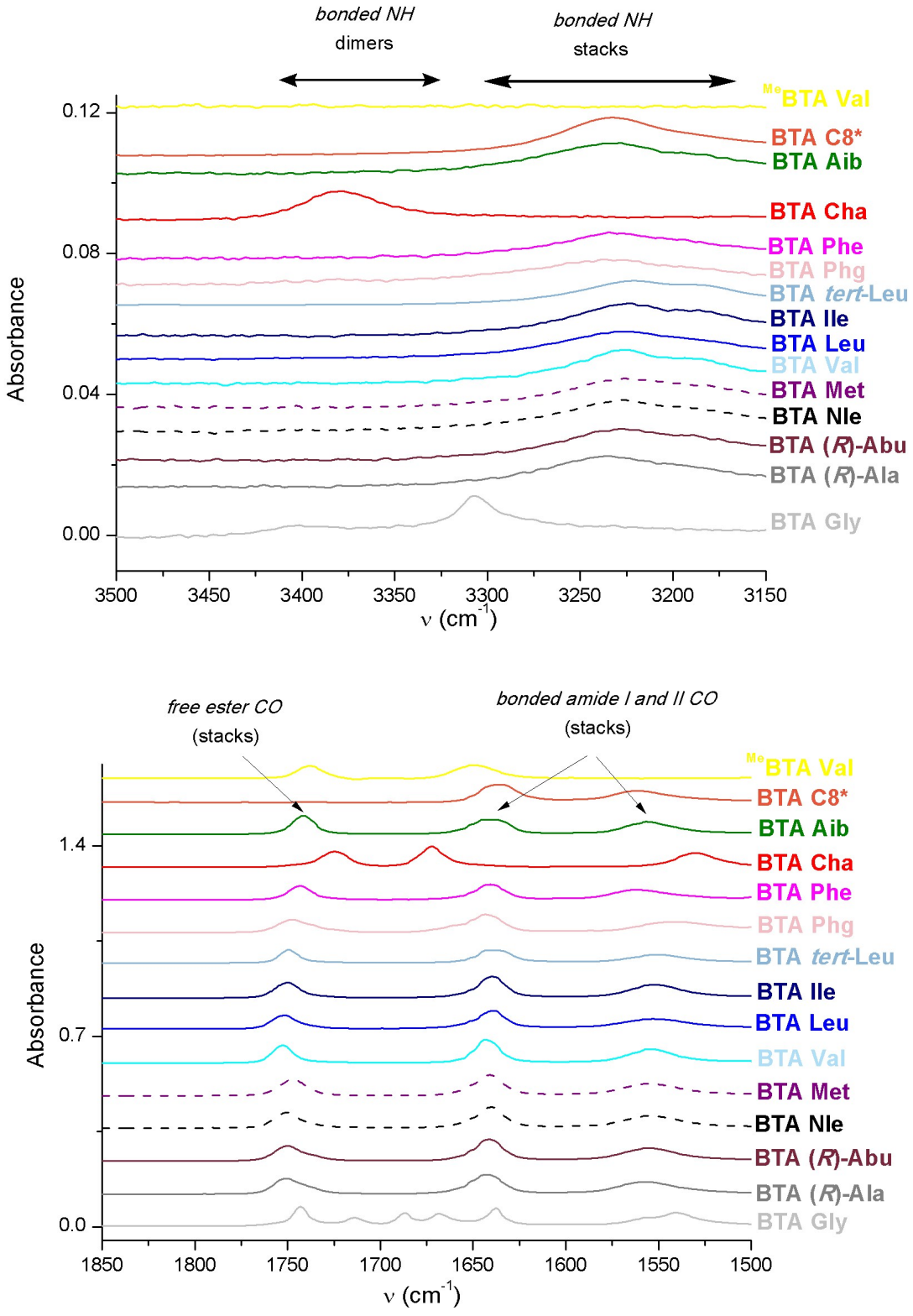

Figure S6. FT-IR spectra of ester BTAs and **BTA C8*** in the bulk at 20°C (ATR-FTIR). Zoom on the N-H (top) and C=O (bottom) regions. Spectra are shown with an offset of 0.01 Abs (N-H) and 0.12 Abs (C=O).

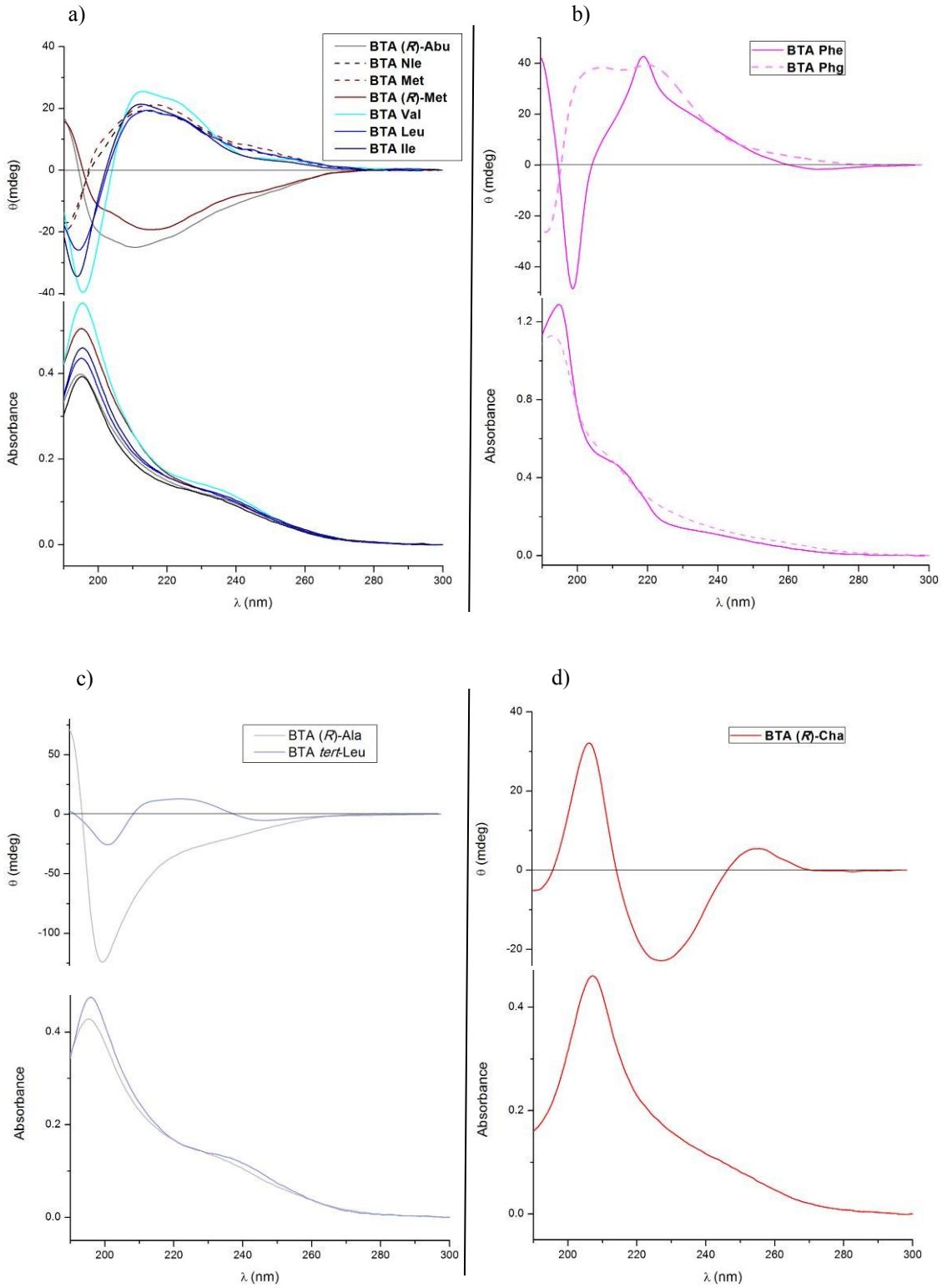

Figure S7. CD spectra of ester BTAs in the bulk (thin films) at 20°C sorted into ester BTAs whose CD spectra is similar to that of **BTA (*R*)-Met** (a, stacks), **BTA Phe** and **BTA Phg** (b, stacks), **BTA (*R*)-Ala** and **BTA *tert*-Leu** (c, stacks) and **BTA (*R*)-Cha** (d, dimers).

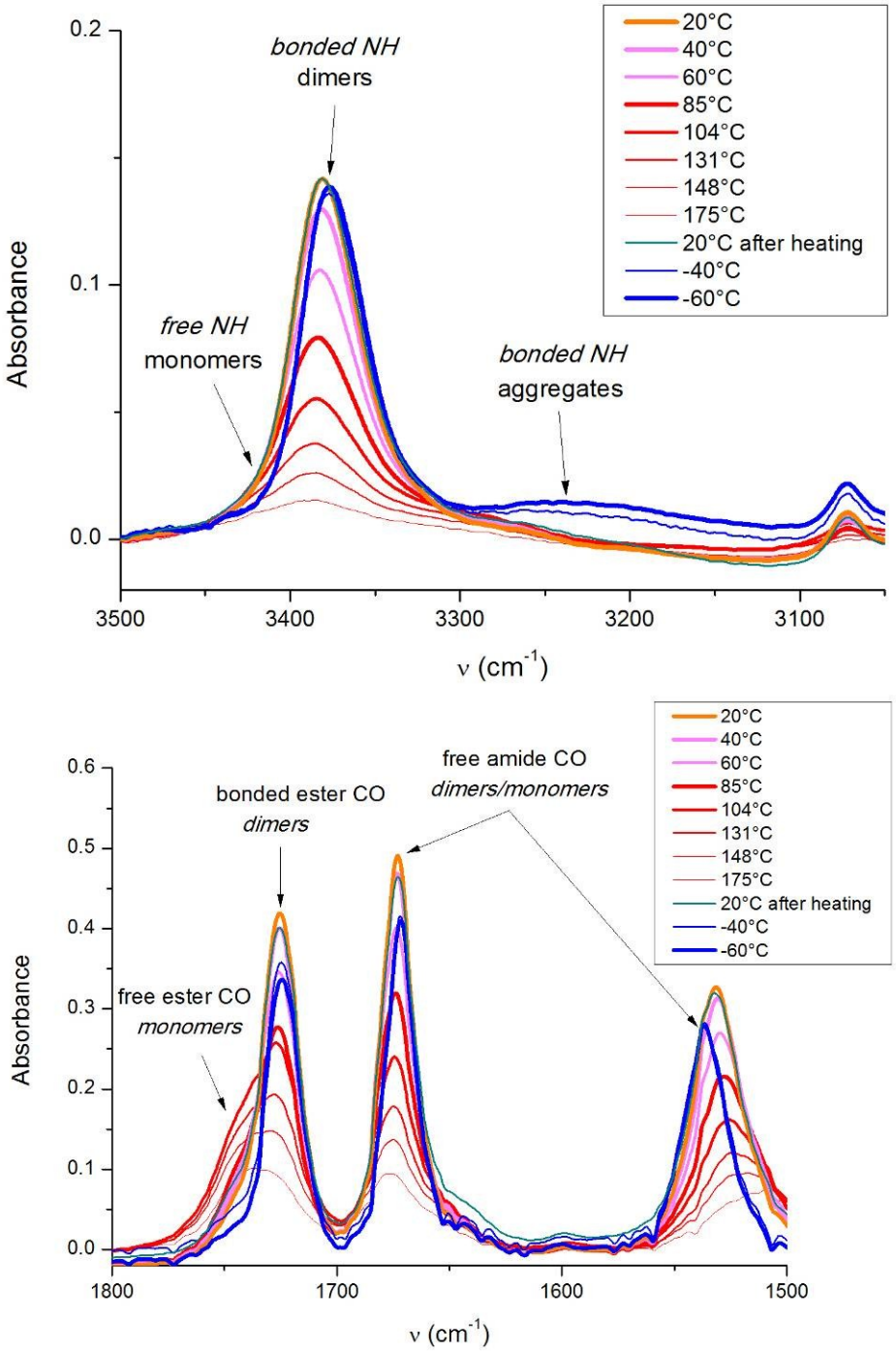

Figure S8. FT-IR spectra of **BTA (*R*)-Cha** neat at various temperatures (KBr plates). Zoom on the N-H (top) and C=O (bottom) regions. The sample is first gradually heated to 175°C then cooled to 20°C and then to -60°C.

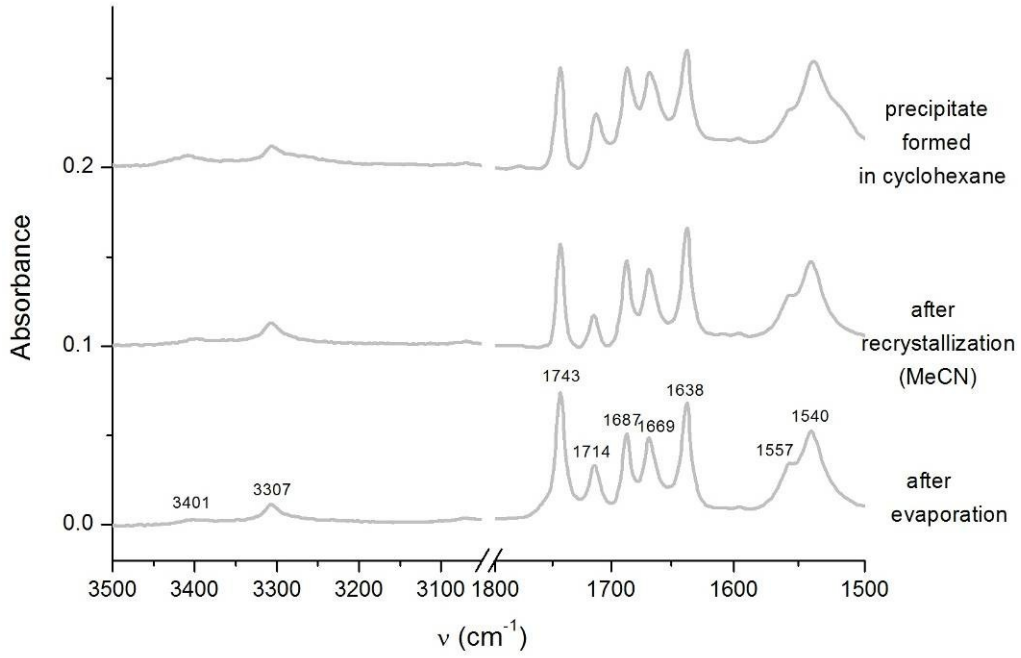

Figure S9. FT-IR spectra of **BTA Gly** in the bulk at 20°C acquired for several samples (ATR-FTIR) corresponding to solids collected after evaporation of the solvent (CH_2Cl_2:AcOEt 1:1), after recrystallization (MeCN) and after filtration of the precipitate obtained after several days from a 20 wt% cyclohexane solution of **BTA Gly**. Spectra are shown with an offset of 0.1 Abs.

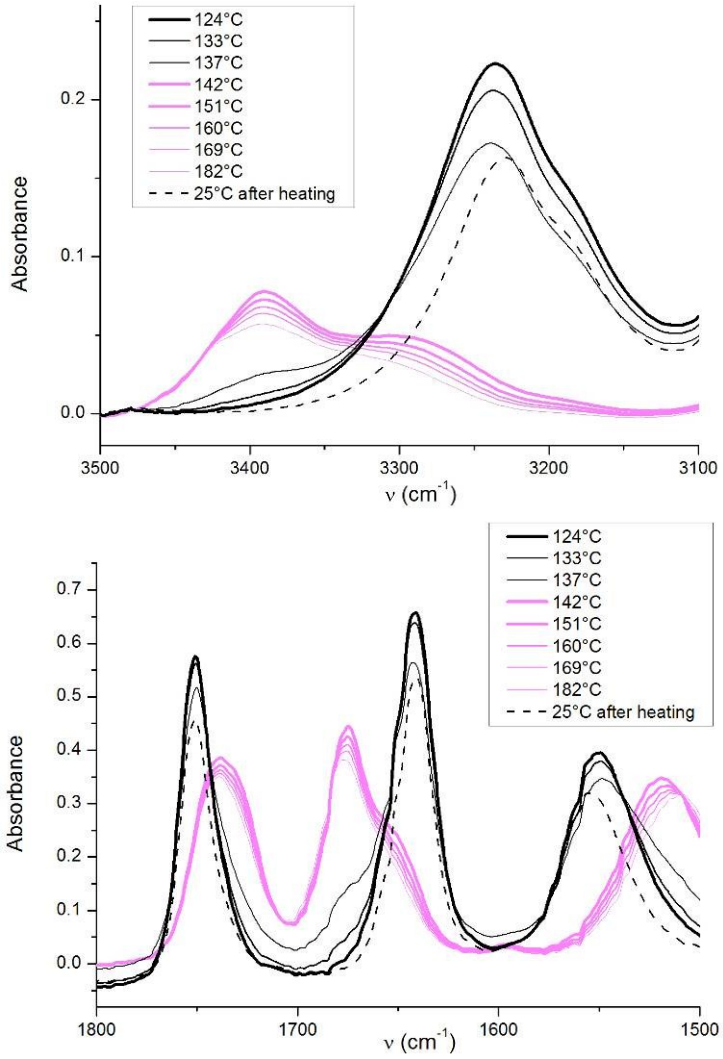

Figure S10. FT-IR spectra of **BTA Nle** in the bulk (KBr plates) above and below its clearing temperature ($T_{cl(DSC)}$=136°C). Zoom on the N-H (top) and C=O (bottom) regions. Heating rate: 1°C.min^{-1}. The lower intensity of the FT-IR signal at 25°C (obtained after heating the solid to 182°C) compared to that at 124°C is likely due loss of matter during the heating process.

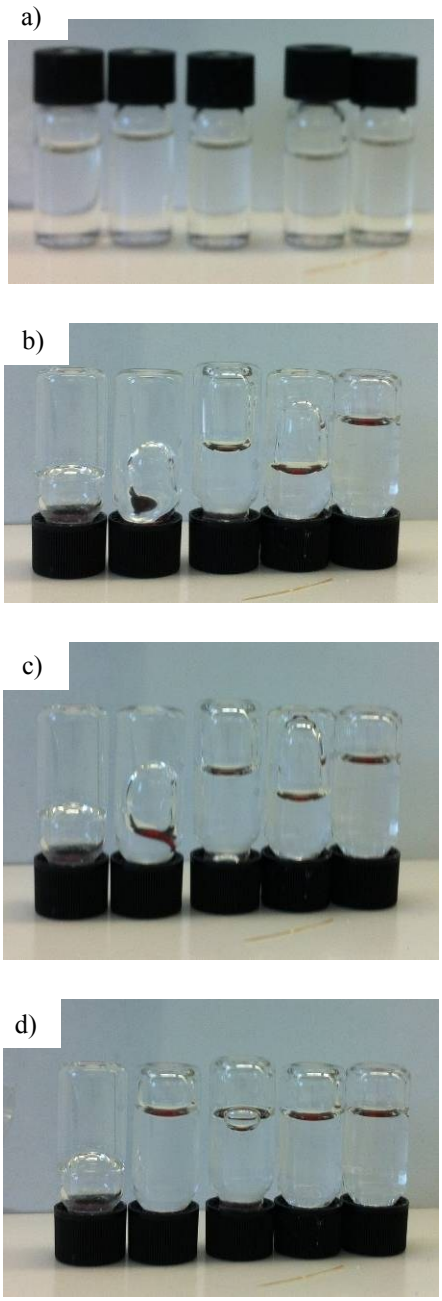

Figure S11. Pictures of the gel/viscous solutions formed by ester BTAs in cyclohexane (20 wt%) at t_0 (a), just after inverting the vials (b), after a few seconds (c) and after 1 minute (d). From the left to the right: **BTA Met**, **BTA Aib**, **BTA Phe**, **BTA (*R*)-Abu** and **BTA (*R*)-Ala**.

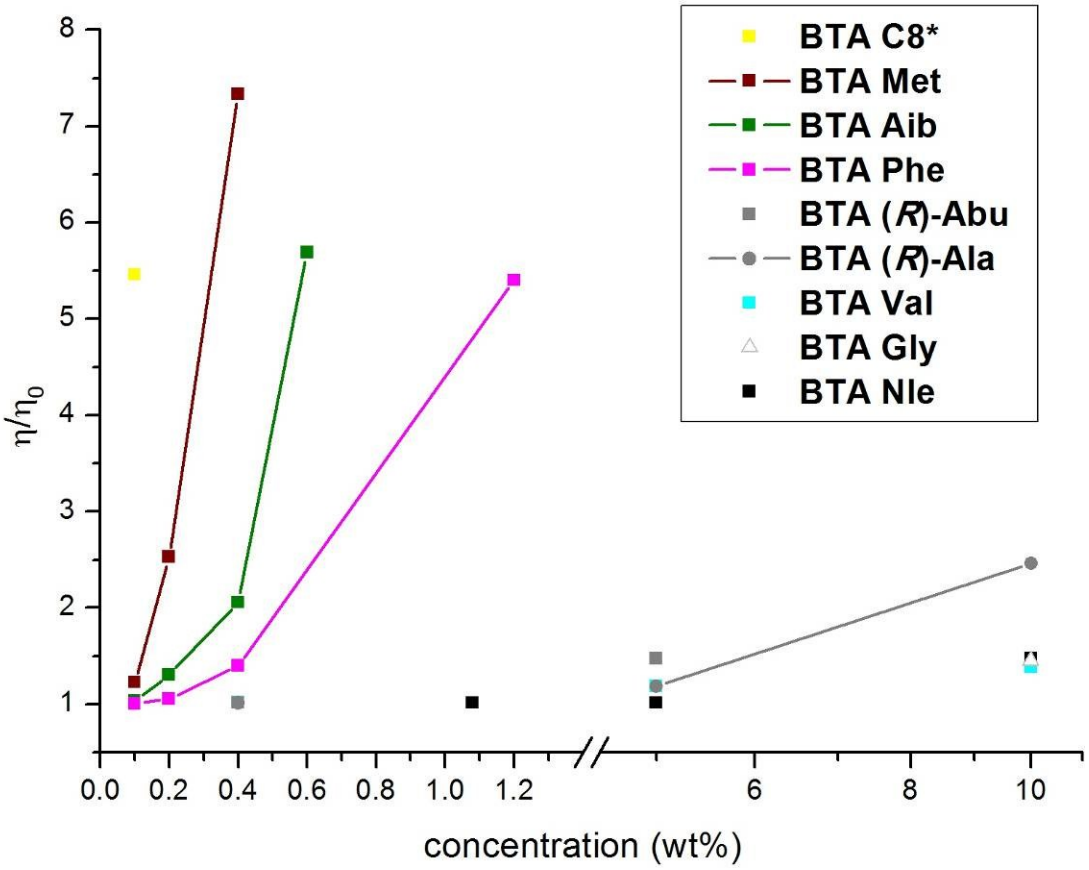

Figure S12. Relative viscosity for a selected set of ester BTAs and **BTA C8*** in cyclohexane *vs* concentration (25°C).

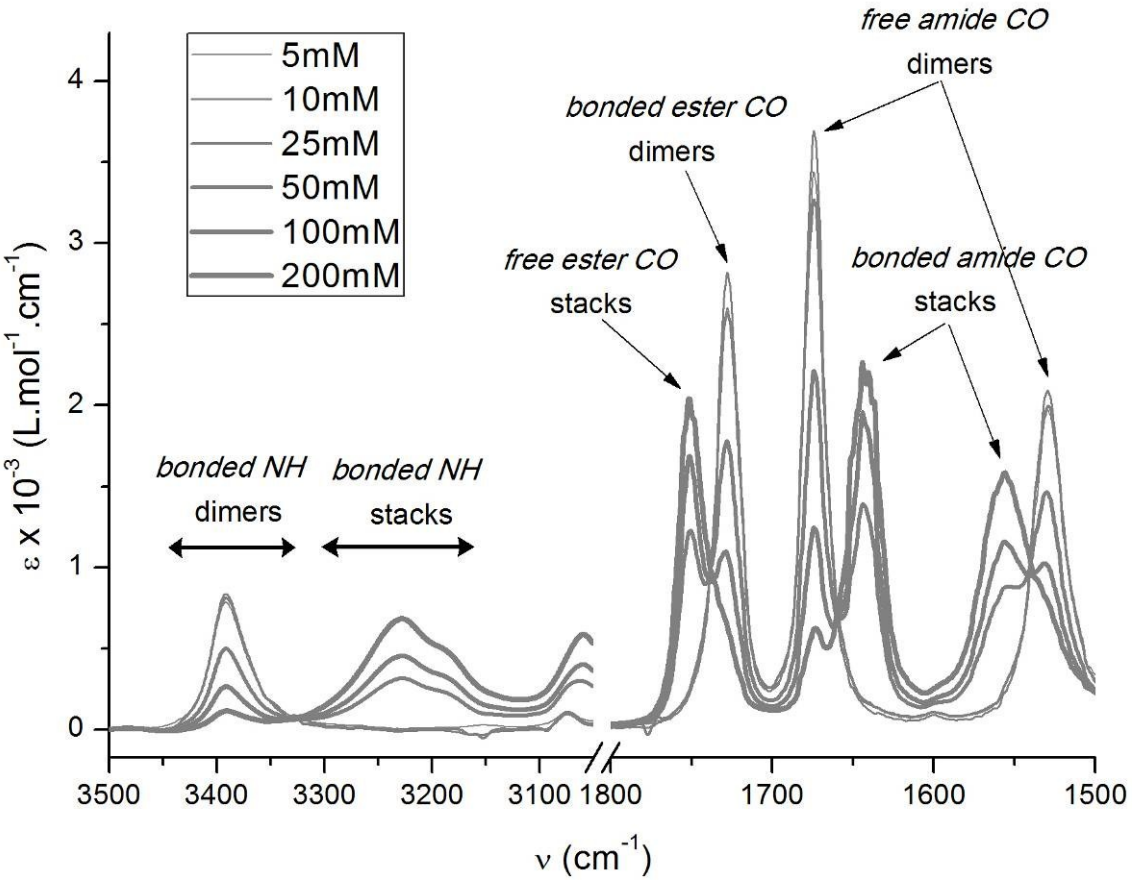

Figure S13. Transition between stacks and dimers for **BTA (*R*)-Abu** in cyclohexane at 20°C as determined by FT-IR analyses. From these data, one can deduce that a 2×10^{-1} M cyclohexane solution of **BTA (*R*)-Abu** (ε_{dimers}=811 L.mol^{-1}.cm^{-1}) contains *ca.* 15% of dimers at 20°C. Critical concentration is estimated to 8×10^{-2} M.

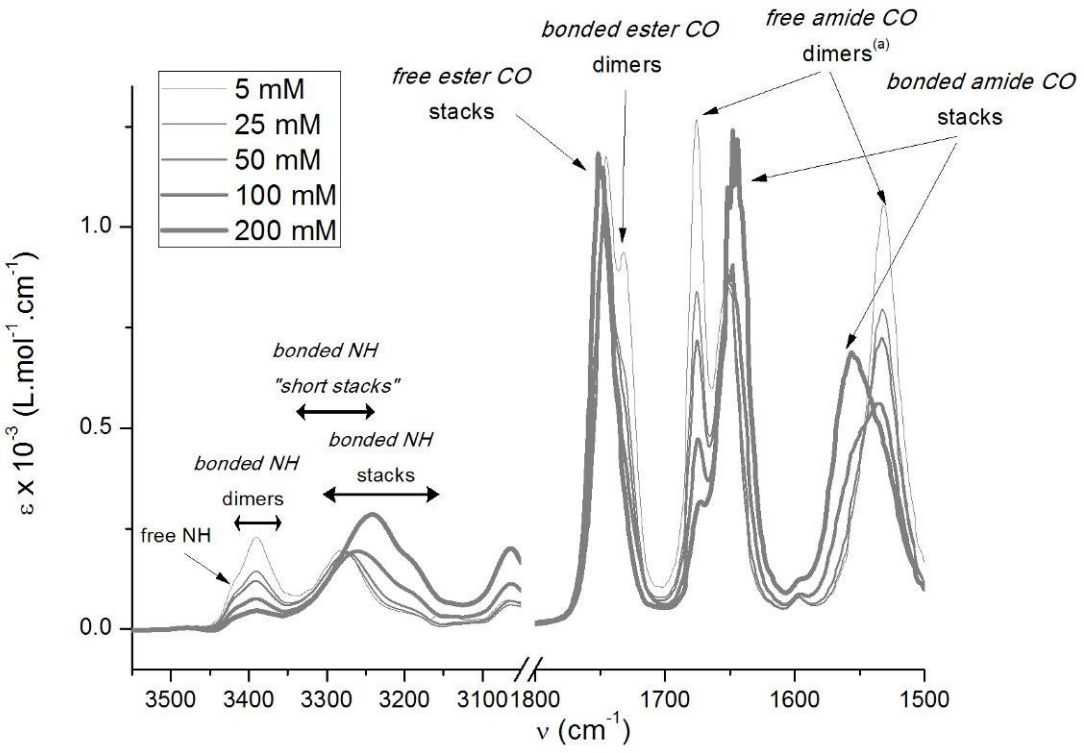

Figure S14. Transition between stacks and dimers for **BTA (*R*)-Ala** in cyclohexane at 20°C as determined by FT-IR analyses. Critical concentration is estimated to 8×10^{-2} M. [(a)] Free amide C=O groups of "short stacks" are also expected to vibrate at these frequencies.

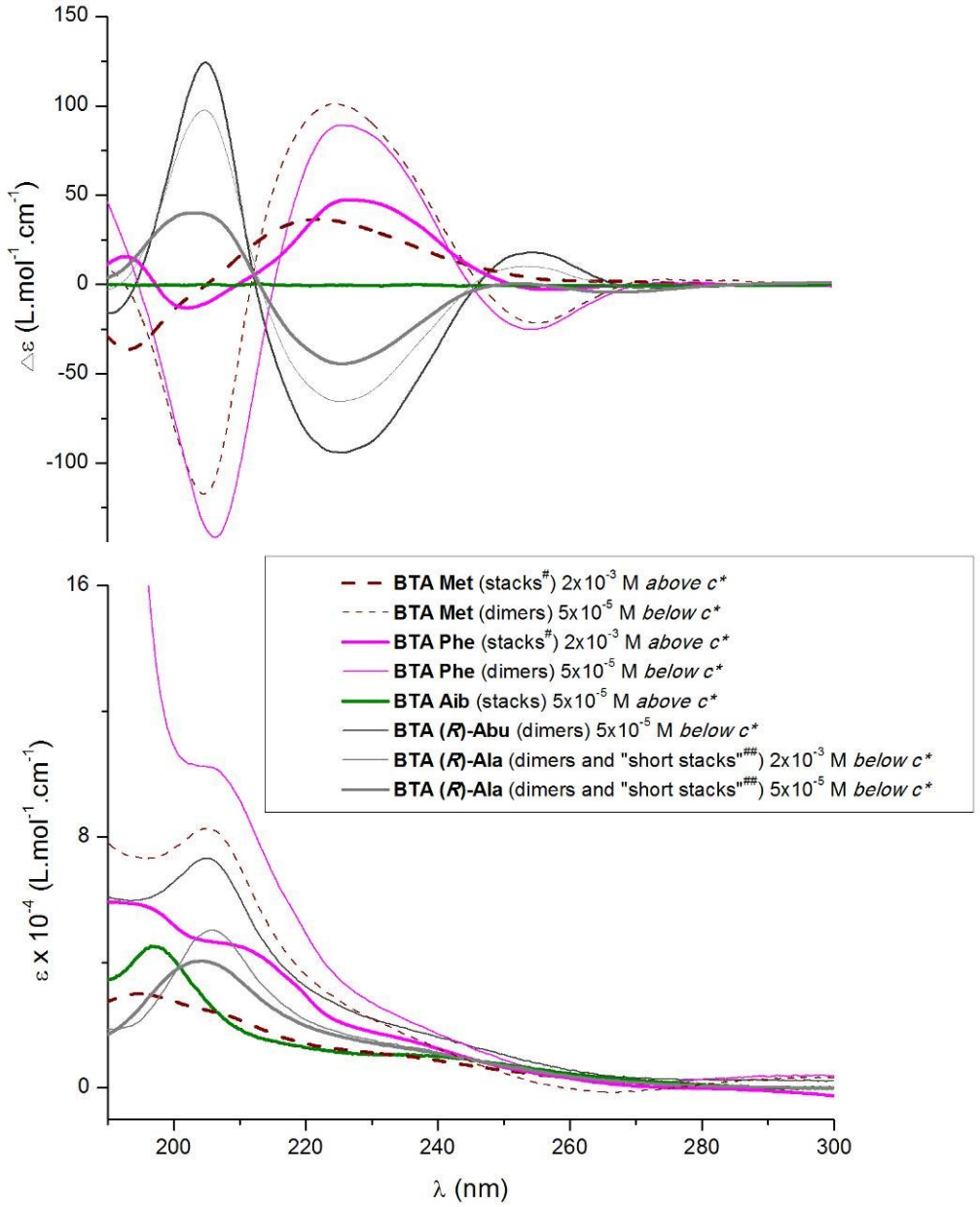

Figure S15. Characterisation by CD (top) and UV-Vis (bottom) of the assemblies formed by **BTA Met**, **BTA Phe**, **BTA Aib**, **BTA (*R*)-Abu** and **BTA (*R*)-Ala** in cyclohexane at 20°C

[#]At 2×10^{-3} M in cyclohexane, **BTA Met** and **BTA Phe** predominantly exist as stacks but *ca.* 22% and 28% of dimers, respectively, are also present as determined by FT-IR analyses (Fig. S21).

[##] For **BTA (*R*)-Ala**, the CD signals are not consistent with the presence of dimers as the only species and in accordance with FT-IR, SANS and ^{1}H NMR analyses we surmise that **BTA (*R*)-Ala** exists as a mixture of dimers and "short stacks" at these concentrations.

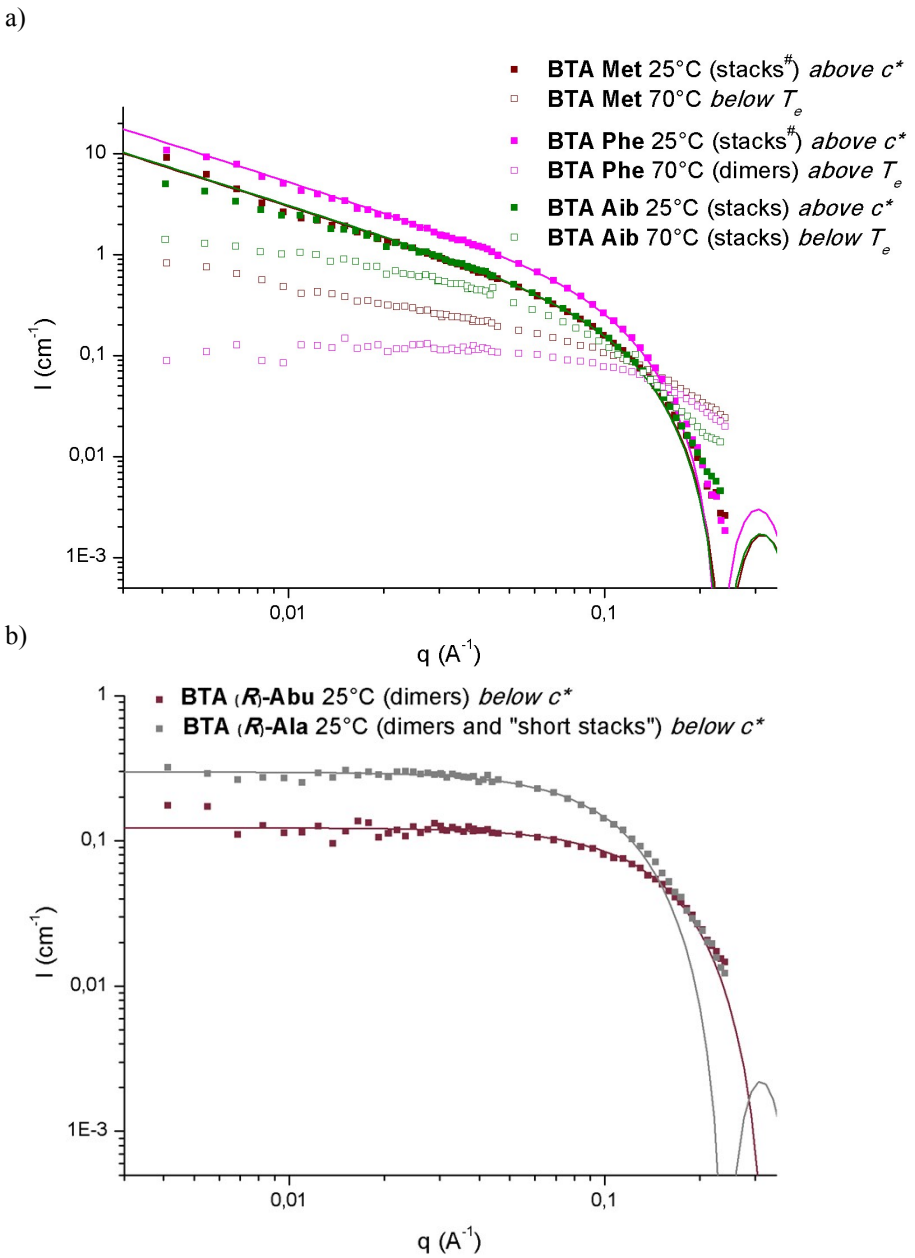

Figure S16. Characterisation by SANS of the assemblies formed by **BTA Met** (1 wt%, 9.6×10^{-3} M), **BTA Phe** (1 wt%, 9.2×10^{-3} M), **BTA Aib** (0.6 wt%, 6.1×10^{-3} M) at 25°C and 70°C (a) and by **BTA (*R*)-Abu** (1 wt%, 1.1×10^{-2} M) and **BTA (*R*)-Ala** (1 wt%, 1.1×10^{-2} M) in C_6D_{12} at 25°C (b).

#At 1 wt%, **BTA Met** and **BTA Phe** predominantly exist as stacks but *ca.* 5% and 7% of dimers, respectively, are also present as determined by FT-IR analyses (Fig. S21).

The curves at 25°C are fitted according to the form factor for rigid rods with a circular cross section and a uniform scattering length density for **BTA Met**, **BTA Phe** and **BTA Aib** or for spheres with a uniform scattering length density for **BTA (*R*)-Abu** and **BTA (*R*)-Ala**. At 70°C, the SANS data are not fitted but one can observe that the cylindrical objects formed by **BTA Met** and **BTA Aib** are shorter while **BTA Phe** forms dimers as the dominant species at this temperature.

Results of the fits (cylindrical objects): r=15.8 Å, 16.5 Å and 16.2 Å for **BTA Met**, **BTA Phe** and **BTA Aib** respectively.

Results of the fits (spheres): r=13.5 Å, M=1850 g.mol^{-1} and $M_{spherical\ object}/M_{monomer}$=1.9 for **BTA (*R*)-Abu**. r=18.5 Å, M=4500 g.mol^{-1} and $M_{spherical\ object}/M_{monomer}$=4.8 for **BTA (*R*)-Ala**.

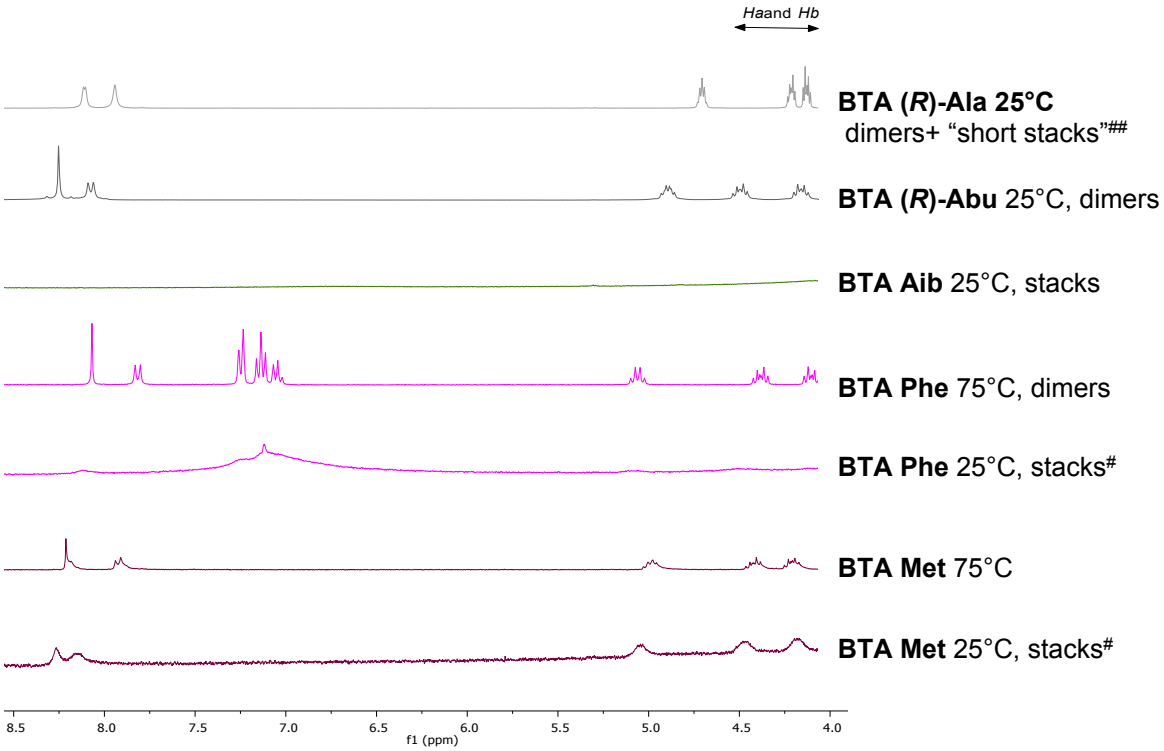

Figure S17. Characterisation by ^{1}H NMR of the assemblies formed by **BTA Met** (5.1×10^{-3} M), **BTA Phe** (9.2×10^{-3} M), **BTA Aib** (10×10^{-3} M), **BTA (*R*)-Abu** (10×10^{-3} M) and **BTA (*R*)-Ala** (10×10^{-3} M) in C_6D_{12} (25°C). Zoom on the region between 3.5 and 9.0 ppm. Diastereotopic protons *Ha* and *Hb* are characteristic peaks for the dimers whilst broad peaks are observed for stacks.

[#] **BTA Met** and **BTA Phe** predominantly exist as stacks but *ca.* 11% and 7% of dimers, respectively, are also present as determined by FT-IR analyses (Fig. S21).

[##] For **BTA (*R*)-Ala**, the NMR signals resemble those characteristic of dimers but, based on other spectroscopic and scattering analyses, we surmise that these signals likely correspond to average signals related to dimers and "short stacks" in fast exchange on the NMR timescale.

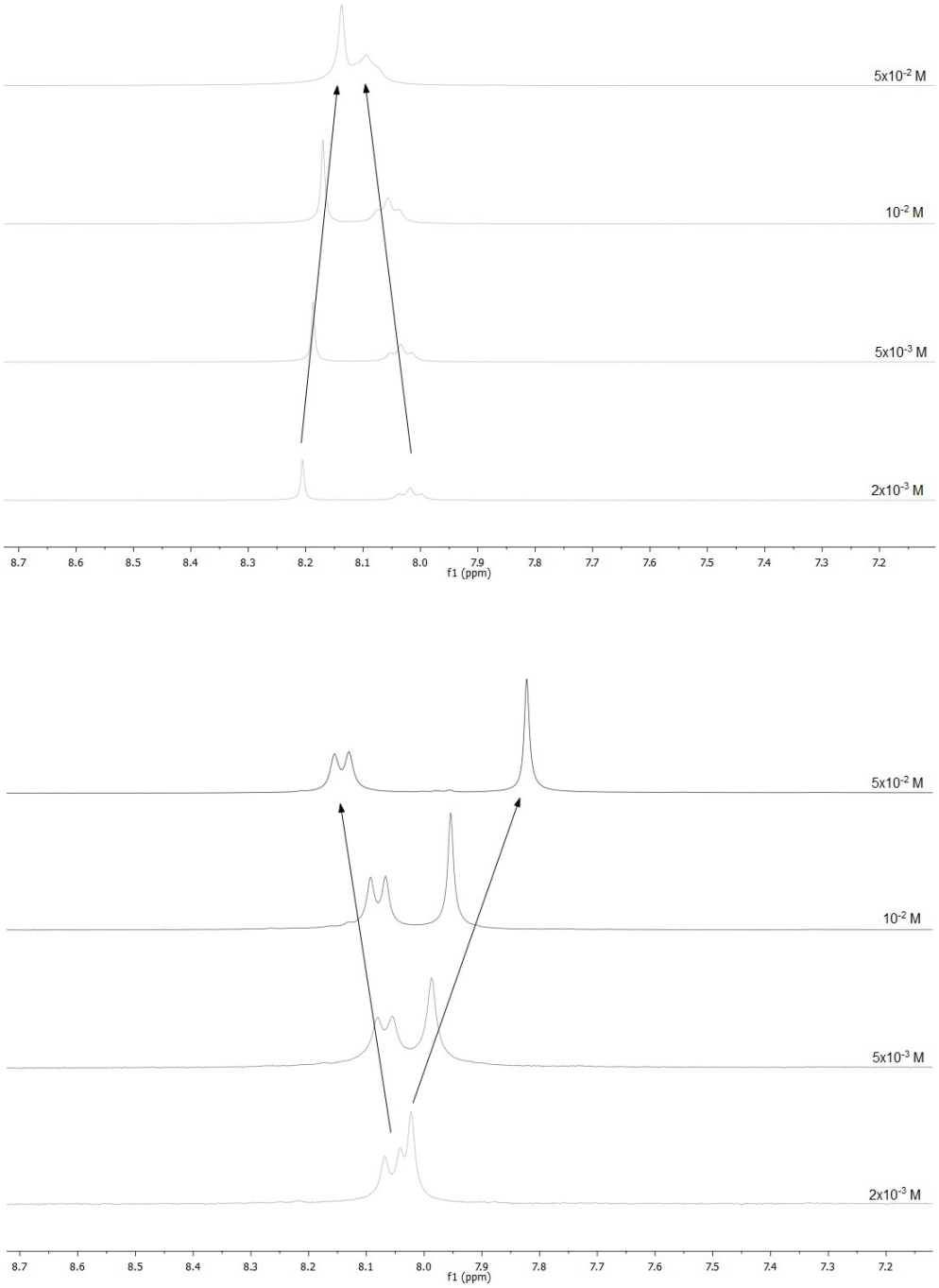

Figure S18. Characterisation by ^{1}H NMR of the assemblies (mixture of dimers and "short stacks") formed by **BTA (*R*)-Ala** (bottom) and **BTA Gly** (top) in C_6D_{12} (25°C). Zoom on the region corresponding to aromatic and N-H protons. Arrows indicate that aromatic protons are upfield shifted while N-H protons are deshielded upon increasing the concentration.

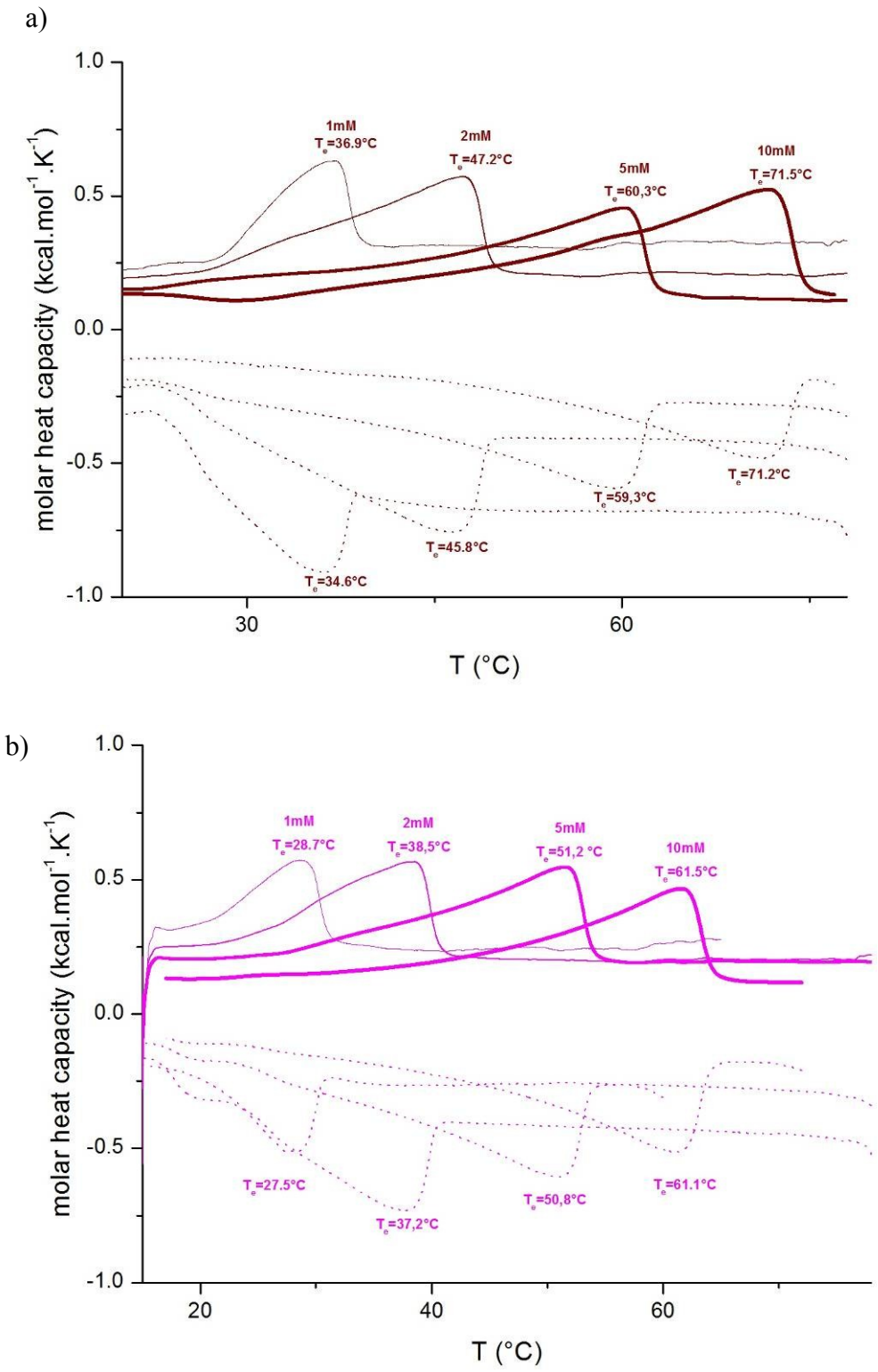

Figure S19. Transition between stacks and dimers for **BTA Met** (a) and **BTA Phe** (b) in cyclohexane at 1.0×10^{-3} M, 2.0×10^{-3} M, 5.0×10^{-3} M and 10.0×10^{-3} M as determined by high-sensitivity DSC. Heating (continuous line) and cooling (dotted line) runs are acquired between 20°C and 80°C (1°C.min^{-1}). T_e is determined at the maximum of the endothermal peak.[9]

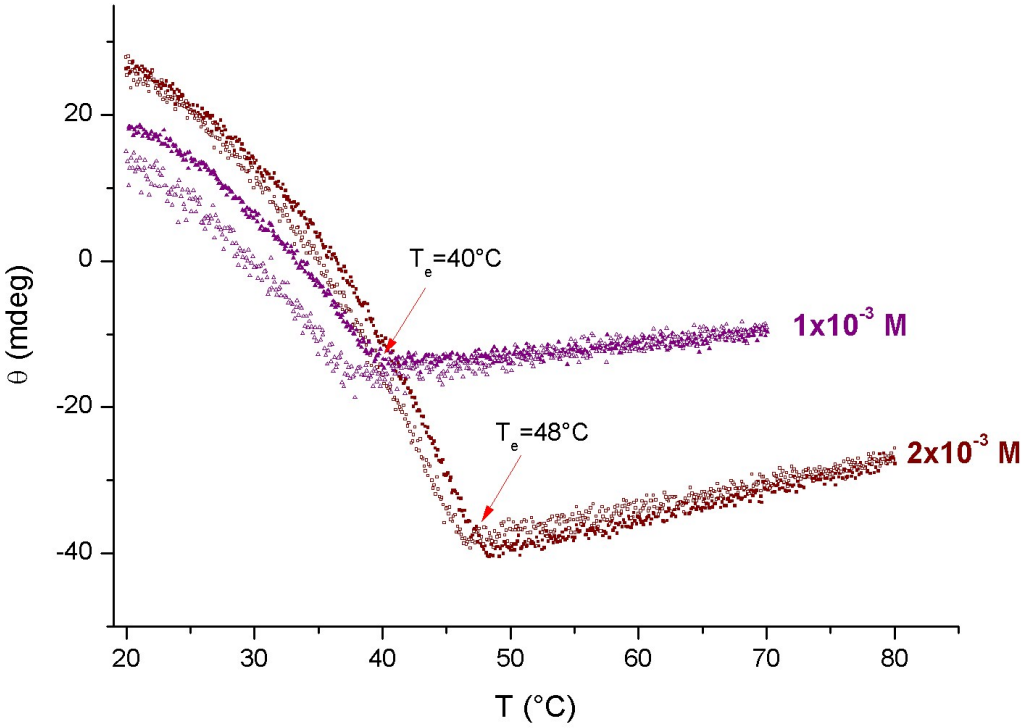

Figure S20. Transition between stacks and dimers for **BTA Met** in cyclohexane as determined by VT-CD. Heating (full symbol) and cooling (empty symbol) experiments are performed between 20°C and 80°C (1°C.min^{-1}). The ellipticity is measured at 255 nm. At λ=255nm stacks exhibit a positive Cotton effect while that of dimers is negative (see full spectra for **BTA Met** in Fig. S15). The elongation temperature is determined as the temperature for which the CD signal stops to decrease.[9]

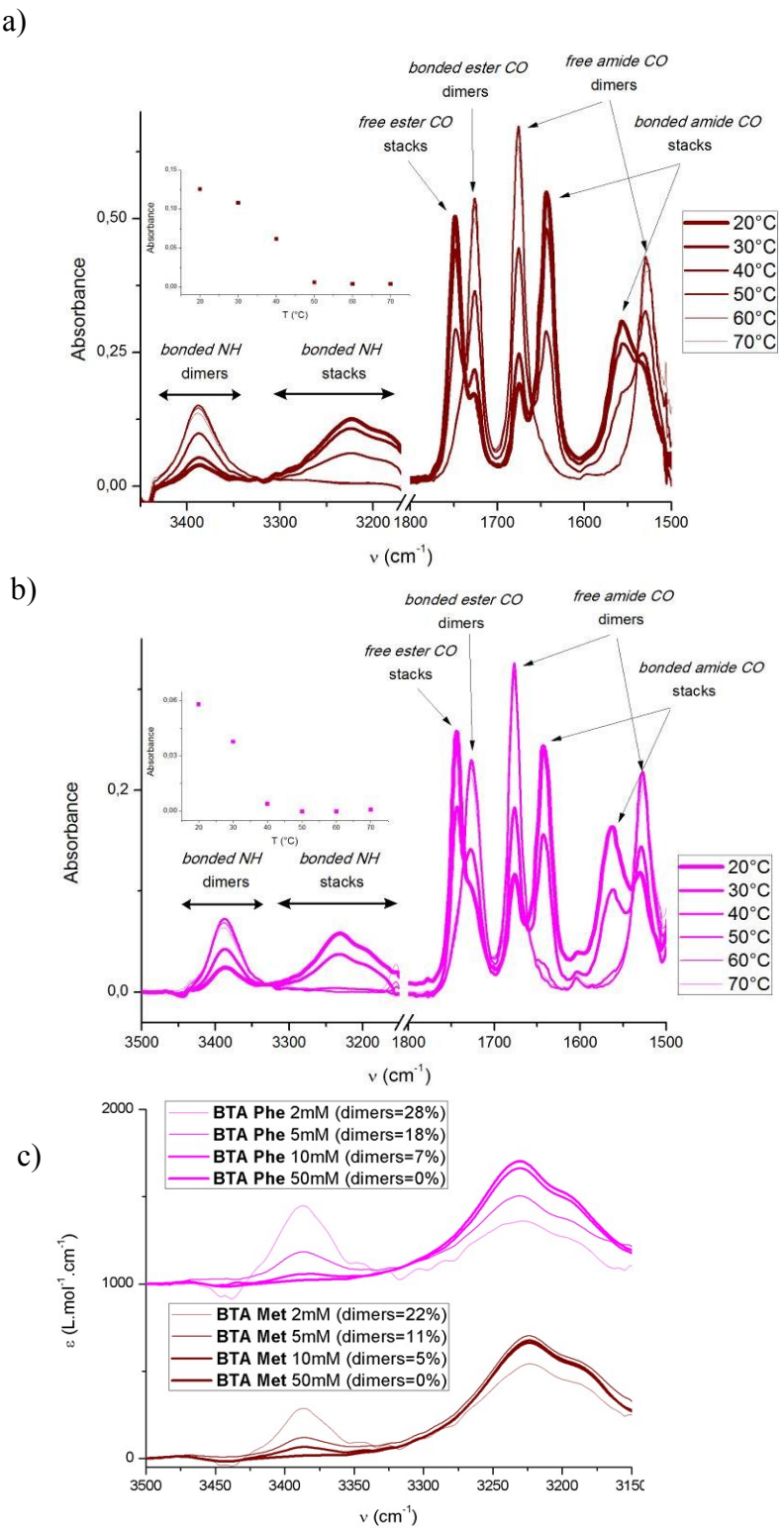

Figure S21. Transition between stacks and dimers for **BTA Met** (a) and **BTA Phe** (b) in cyclohexane at 2×10^{-3} M as followed by VT FT-IR analyses. At 20°C **BTA Met** and **BTA Phe** predominantly exists as stacks while only dimers are present at 50°C and 60°C for **BTA Phe** and **BTA Met** respectively. Insets: FT-IR absorbance (ν=3223 cm^{-1} and ν =3230 cm^{-1} for **BTA Met** and **BTA Phe** respectively) plotted as a function of the temperature. From these data, one can deduce the amount of dimers in cyclohexane solutions of **BTA Met** (ε_{dimers}=894 $L.mol^{-1}.cm^{-1}$) and **BTA Phe** (ε_{dimers}=864 $L.mol^{-1}.cm^{-1}$) at different concentrations at 20°C (c). **BTA Phe** spectra are shown with an offset of 1000 $L.mol^{-1}.cm^{-1}$.

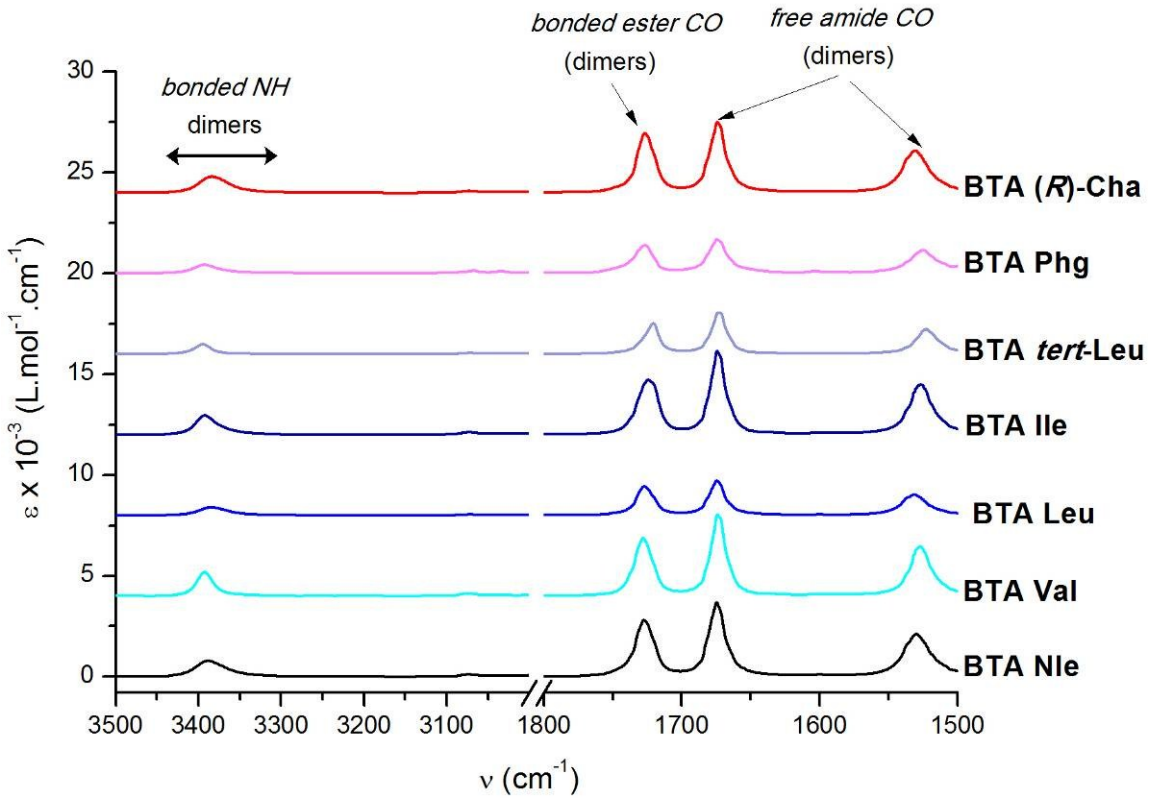

Figure S22. Characterisation by FT-IR of the assemblies (dimers only) formed by **BTA Nle**, **BTA Val**, **BTA Leu**, **BTA Ile**, **BTA *tert*-Leu**, **BTA Phg** and **BTA (*R*)-Cha** in cyclohexane at 20°C (5×10^{-2} M). Spectra are shown with an offset of 4000 $L.mol^{-1}.cm^{-1}$.

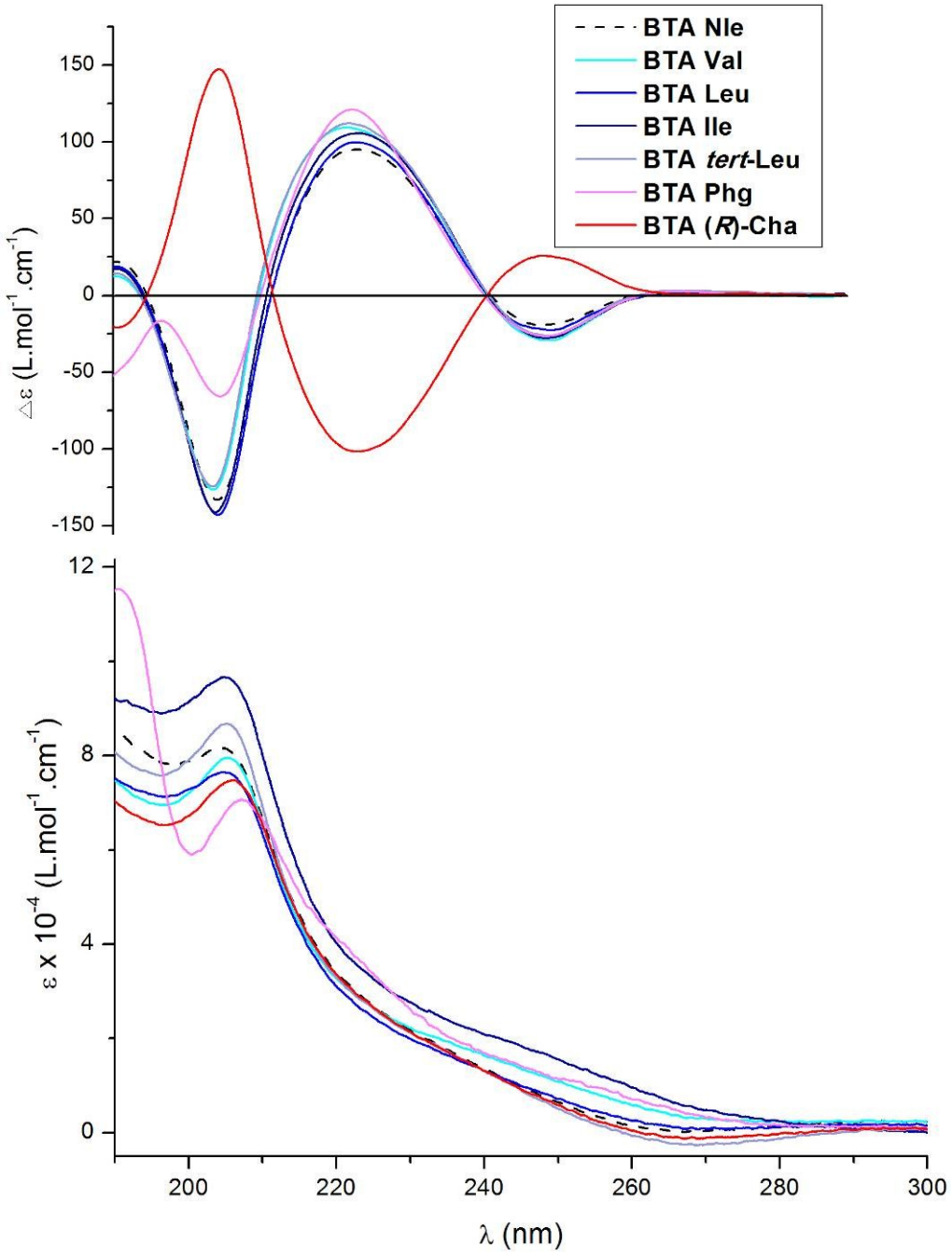

Figure S23. Characterisation by CD and UV-Vis of the assemblies formed by **BTA Nle**, **BTA Val**, **BTA Leu**, **BTA Ile**, **BTA *tert*-Leu**, **BTA Phg** and **BTA (*R*)-Cha** in cyclohexane at 20°C (5×10^{-5} M). All the CD and UV-Vis signals are diagnostic of the dimers.

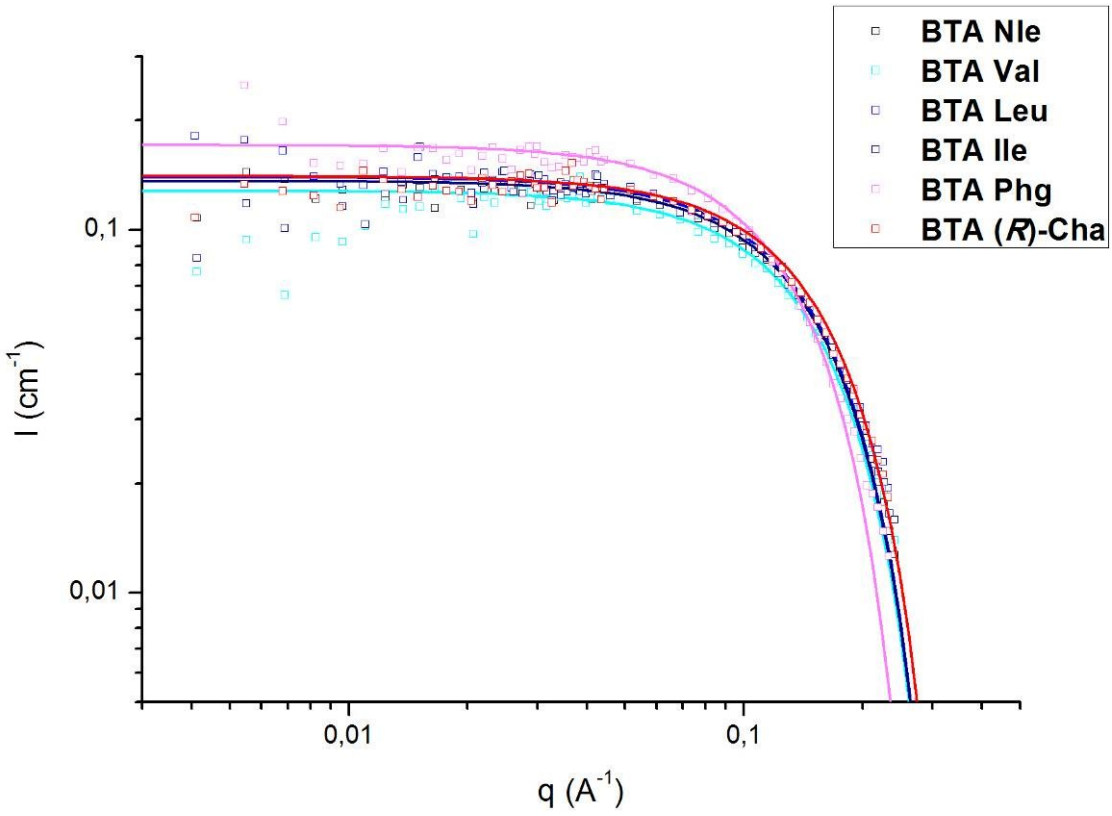

Figure S24. Characterisation by SANS (25°C) of the dimers formed by **BTA Nle** (1 wt%, 10.1×10^{-3} M), **BTA Val** (1 wt%, 10.1×10^{-3} M), **BTA Leu** (0.6 wt%, 10.1×10^{-3} M), **BTA Ile** (1 wt%, 10.1×10^{-3} M), **BTA Phg** (1 wt%, 9.5×10^{-3} M) and **BTA (*R*)-Cha** (1 wt%, 8.9×10^{-3} M) in C_6D_{12}. The curves are fitted according to the form factor for spheres with a uniform scattering length density. Results of the fits:

BTA Nle: r=13.5 Å, M=2000 g.mol^{-1}, $M_{spherical\ object}/M_{monomer}$=1.9

BTA Val: r=13.5 Å, M=1900 g.mol^{-1}, $M_{spherical\ object}/M_{monomer}$=1.9

BTA Leu: r=13.5 Å, M=2050 g.mol^{-1}, $M_{spherical\ object}/M_{monomer}$=1.9

BTA Ile: r=13.5 Å, M=2000 g.mol^{-1}, $M_{spherical\ object}/M_{monomer}$=1.9

BTA Phg: r=15.5 Å, M=2900 g.mol^{-1}, $M_{spherical\ object}/M_{monomer}$=2.6

BTA (*R*)-Cha: r=13.0 Å, M=2100 g.mol^{-1}, $M_{spherical\ object}/M_{monomer}$=1.8

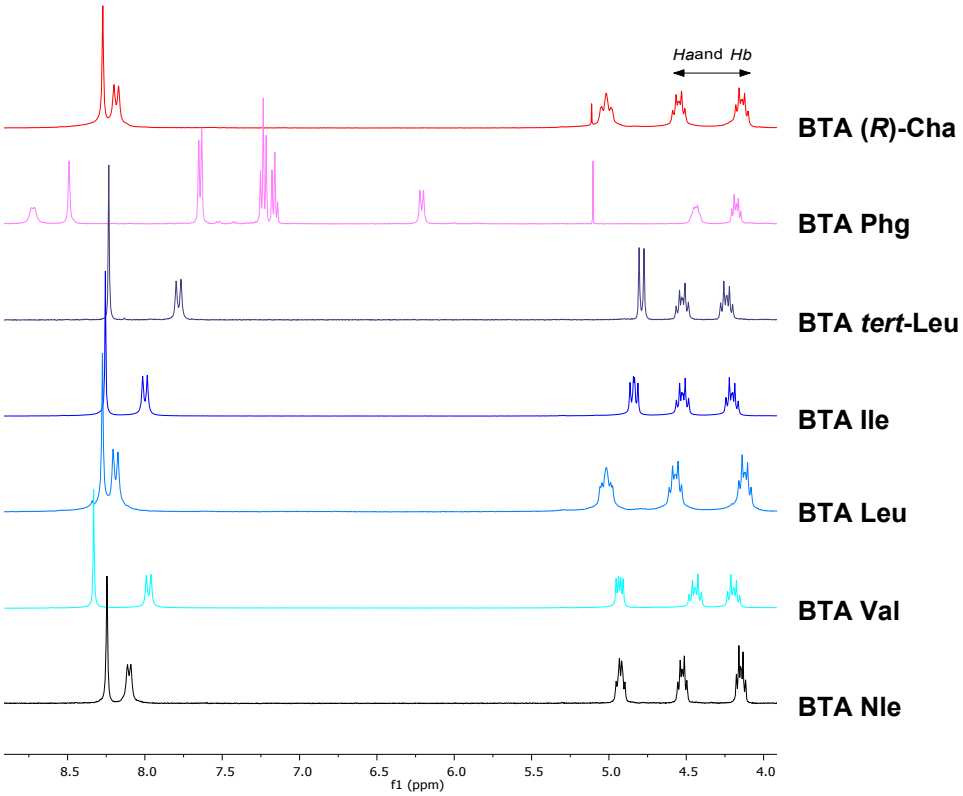

Figure S25. Characterisation by ^{1}H NMR of the dimers formed by **BTA Nle**, **BTA Val**, **BTA Leu**, **BTA Ile**, **BTA *tert*-Leu**, **BTA Phg** and **BTA (*R*)-Cha** in C_6D_{12} (10^{-2} M, 25°C). Zoom on the region between 3.0 and 9.5 ppm. Diastereotopic protons *Ha* and *Hb* are characteristic peaks for the ester-bonded dimers. Singlet at 5.1 ppm in the spectra of **BTA Phg** and **BTA (*R*)-Cha** corresponds to residual CH_2Cl_2.

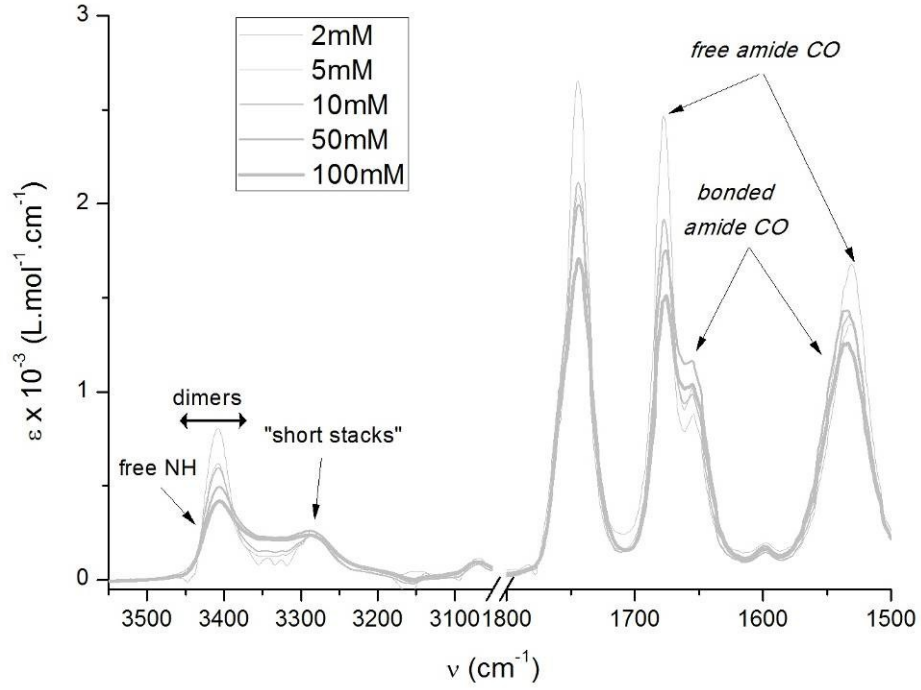

Figure S26. Characterisation by FT-IR of the assemblies (dimers and "short stacks") formed by **BTA Gly** in cyclohexane at 20°C.

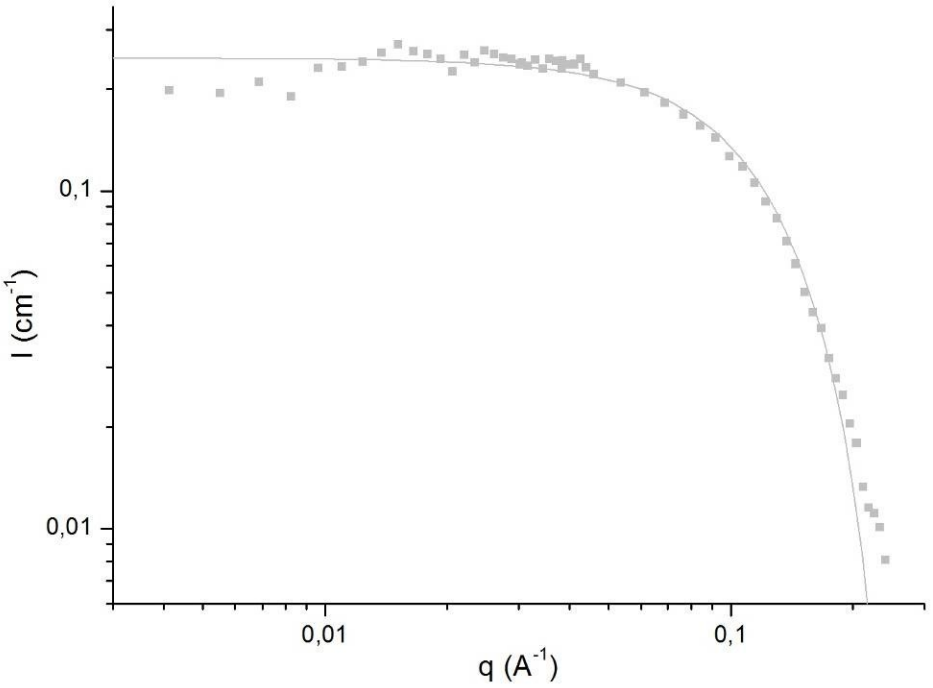

Figure S27. Characterisation by SANS (25°C) of the assemblies formed by **BTA Gly** (1 wt%, 12.0×10^{-3} M) in C_6D_{12}. The curve is fitted according to the form factor for spheres with a uniform scattering length density yielding the following values: r=17.0 Å, M=4000 g.mol^{-1} and $M_{spherical\ object}/M_{monomer}$=4.5.

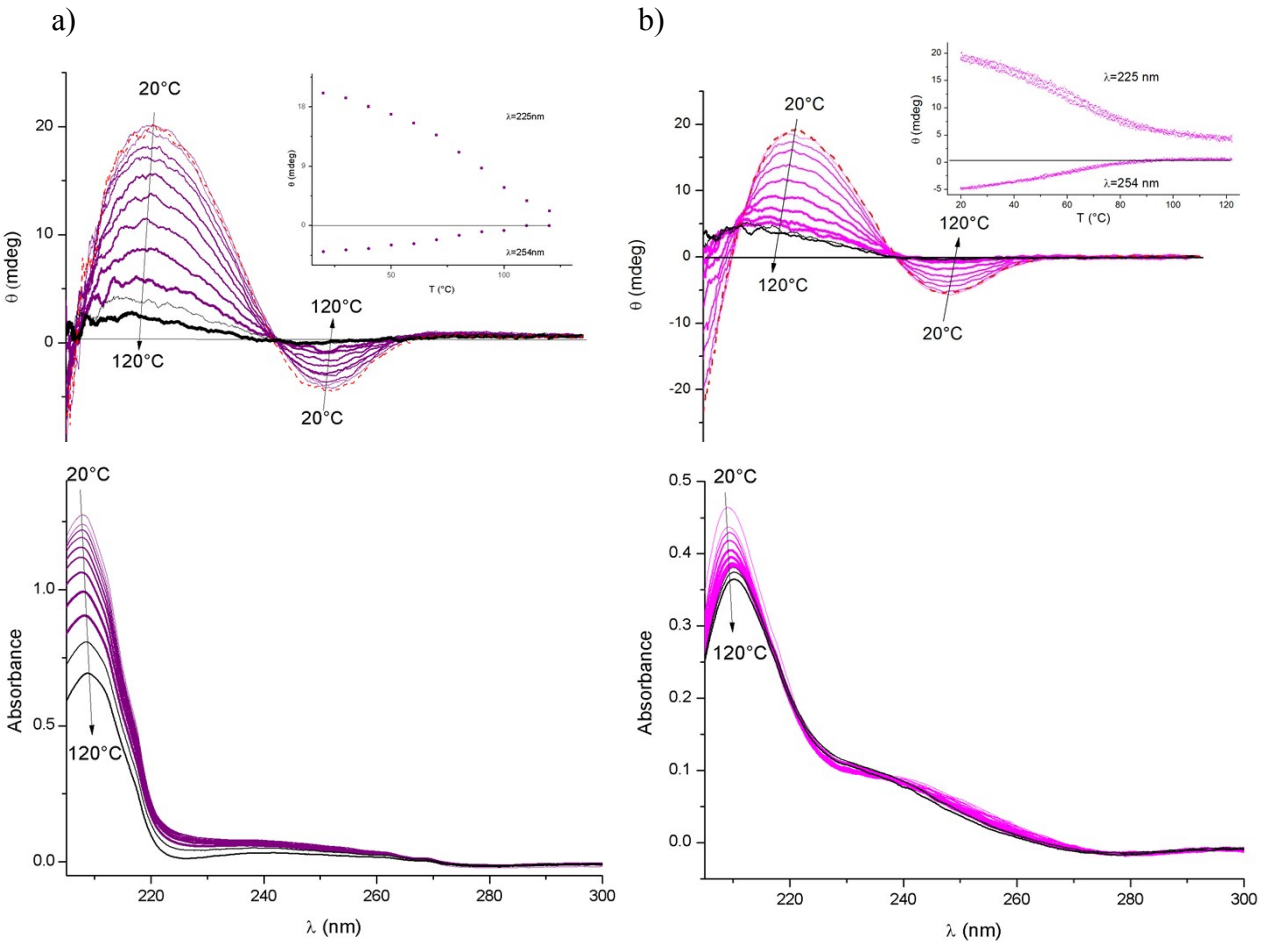

Figure S28. Transition between dimers and monomers for **BTA Met** (a) and **BTA Phe** (b) as determined by CD (top) and UV (bottom) experiments performed between 20°C and 120°C in methylcyclohexane ($c=7\times10^{-6}$ M). Inset: plot of the ellipticity measured at 225 nm and 254 nm against the temperature (for **BTA Phe** full and empty squares correspond to heating and cooling runs respectively); 1°C.min^{-1} for all. Spectra in dashed red lines correspond to spectra obtained upon returning to the initial temperature (20°C). The transition temperature (*T***) between dimers and monomers is determined at the point of inflection of the curve.

References.

1. A. Desmarchelier, M. Raynal, P. Brocorens, N. Vanthuyne and L. Bouteiller, *Chem. Commun.*, 2015, **51**, 7397-7400.
2. A. Desmarchelier, X. Caumes, M. Raynal, A. Vidal-Ferran, P. W. N. M. van Leeuwen and L. Bouteiller, *J. Am. Chem. Soc.*, 2016, **138**, 4908-4916.
3. P. J. M. Stals, M. M. J. Smulders, R. Martín-Rapún, A. R. A. Palmans and E. W. Meijer, *Chem. Eur. J.*, 2009, **15**, 2071-2080.
4. S. L. Mayo, B. D. Olafson and I. W. A. Goddard, *J. Phys. Chem.*, 1990, **94**, 8897-8909.
5. H. Sun, *J. Comput. Chem.*, 1994, **15**, 752-768.
6. H. Sun, *Macromolecules*, 1995, **28**, 701-712.
7. S. A. Nose, *Mol. Phys.*, 1984, **52**, 255-268.
8. Gaussian 09, Revision **E.01**, M. J. Frisch, G. W. Trucks, H. B. Schlegel, G. E. Scuseria, M. A. Robb, J. R. Cheeseman, G. Scalmani, V. Barone, B. Mennucci, G. A. Petersson, H. Nakatsuji, M. Caricato, X. Li, H. P. Hratchian, A. F. Izmaylov, J. Bloino, G. Zheng, J. L. Sonnenberg, M. Hada, M. Ehara, K. Toyota, R. Fukuda, J. Hasegawa, M. Ishida, T. Nakajima, Y. Honda, O. Kitao, H. Nakai, T. Vreven, J. A. Montgomery, Jr., J. E. Peralta, F. Ogliaro, M. Bearpark, J. J. Heyd, E. Brothers, K. N. Kudin, V. N. Staroverov, R. Kobayashi, J. Normand, K. Raghavachari, A. Rendell, J. C. Burant, S. S. Iyengar, J. Tomasi, M. Cossi, N. Rega, J. M. Millam, M. Klene, J. E. Knox, J. B. Cross, V. Bakken, C. Adamo, J. Jaramillo, R. Gomperts, R. E. Stratmann, O. Yazyev, A. J. Austin, R. Cammi, C. Pomelli, J. W. Ochterski, R. L. Martin, K. Morokuma, V. G. Zakrzewski, G. A. Voth, P. Salvador, J. J. Dannenberg, S. Dapprich, A. D. Daniels, Ö. Farkas, J. B. Foresman, J. V. Ortiz, J. Cioslowski, and D. J. Fox, *Gaussian, Inc., Wallingford CT*, 2009.
9. M. M. J. Smulders, A. P. H. J. Schenning and E. W. Meijer, *J. Am. Chem. Soc.*, 2008, **130**, 606-611.
10. M. Prashad, D. Har, B. Hu, H. Y. Kim, O. Repic and T. J. Blacklock, *Org. Lett.*, 2003, **5**, 125.

Synthesis.

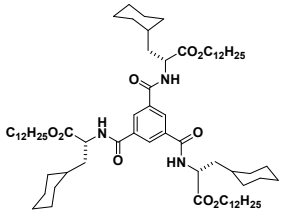

BTA (*R*)-Cha

Tri-N-[(*R*)-(1-methylene-cyclohexyl)dodecyloxycarbonymethyl]benzene-1,3,5-tricarboxamide (BTA (*R*)-Cha)

Step1: In a Dean-Stark apparatus-mounted two-neck flask, 3-cyclohexyl-(*R*)-Alanine hydrate (3.01 g, 15.7 mmol, 1.0 equiv.) is suspended in toluene (0.11 M, 150 mL), and *p*-TsOH.H_2O (3.58 g, 18.8 mmol, 1.2 equiv.) is added at room temperature. Dodecanol (3.51 g, 18.8 mmol, 1.2 equiv.) is then added, and the resulting slurry is stirred at reflux temperature overnight. After cooling the reaction mixture to room temperature, the solvent is evaporated and the crude reaction mixture is dried under reduced pressure to give a solid. This solid is taken up in *ca.* 70 mL of Et_2O, gently heated to 35°C, and let cool in the freezer (ca. -35°C). The resulting precipitate is quickly filtered under vacuum and washed with cold ether. The white solid is then dried under vacuum to yield the pure ammonium tosylate (7.23 g, 14.1 mmol, 90%). **^{1}H NMR** (300 MHz, DMSO-d6): δ 8.27 (br s, 3H), 7.48 (d, *J* = 7.5 Hz, 2H), 7.12 (d, *J* = 7.7 Hz, 2H), 4.23-4.07 (m, 2H), 4.03 (br s, 1H), 2.29 (s, 3H), 1.74-1.53 (m, 9H), 1.49-1.07 (m, 24H), 0.85 (t, *J* = 6.2 Hz, 3H).

Step2: In a flame-dried round-bottom flask under argon atmosphere, benzene-1,3,5-tricarboxylic acid chloride (1.14 g, 4.3 mmol, 1.0 equiv.) is dissolved in dry DCM (100 mL) at room temperature. The ammonium tosylate (7.20 g, 14.1 mmol, 3.3 equiv.) is then added in one portion, and the resulting mixture is cooled to 0°C with an ice/water bath. Et_3N (4.2 mL, 31.0 mmol, 7.3 equiv.) is then added dropwise, the reaction is let warm to room temperature and stirred for 48h. Brine is then added to the flask, and the crude mixture is extracted thrice with DCM. The combined organic phases are dried over $MgSO_4$, filtered, and the solvent is evaporated under reduced pressure. The resulting solid is taken up as a slurry in a little DCM, and purified on a short column of silica gel (elution: DCM/EtOAc 6:1) to remove salts and impurities (R_f ~ 0.85-0.9). The product is then purified by column chromatography on silica gel, eluting with DCM/EtOAc 95:5 – 75:25 gradient (R_f ~ 0.1–0.2). Two different fractions were collected which after evaporation gave 4.0 g (2.0 g each, 79% total yield) of **BTA (*R*)-Cha** as a gum-like solid. The two samples only differ by the ratio of diastereomers ((*R*,*R*,*S*) and (*S*,*S*,*R*)) relatively to enantiopure **BTA (*R*)-Cha**. The first and second sample contain *ca.* 7% and <2% of diastereomers as determined by NMR and chiral HPLC analyses. Only **BTA (*R*)-Cha** issued from the second fraction was used in this study (*ee*>99%, *de*>99%, see page S35).

^{1}H NMR (300 MHz, acetone-d6): δ 8.48 (s, 3H), 8.25 (d, *J* = 7.8 Hz, 3H), 4.78-4.71 (m, 3H), 4.20–4.07 (m, 6H), 1.94–1.47 (m, 27H), 1.47–1.13 (m, 66H), 1.10–0.93 (m, 6H), 0.88 (t, *J* = 6.9 Hz, 9H) signal corresponding to diastereomers is not observed in this sample (δ 8.50); **^{13}C{^{1}H} NMR** (75 MHz, acetone-d6): δ 173.6, 166.6, 135.9, 129.8, 65.6, 51.9, 39.9, 35.1, 34.3, 33.1, 32.7, 30.4, 30.4, 30.3, 30.3, 30.0,

29.5, 27.2, 27.0, 26.8, 26.7, 23.4, 14.4; **HRMS:** Calculated for $C_{72}H_{124}N_3O_9$ $[M+H]^+$: 1174.9332, found: 1174.9329. IR (solid) see Figure S.5. *ee*>99%, *de*>99% (page S35).

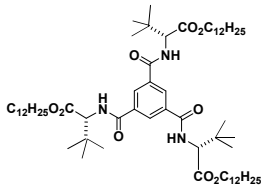

BTA *tert*-Leu

Tri-N-[(*S*)-(tertiobutyl)dodecyloxycarbonymethyl]benzene-1,3,5-tricarboxamide (BTA *tert*-Leu)

Step1: (*S*)-*tert*-Leucine (1.02 g, 7.6 mmol, 1.0 equiv.) in dodecanol (10.0 g) is heated to 60°C, thionyl chloride (0.88 mL, 12.1 mmol, 1.6 equiv.) and the reaction mixture is stirred overnight. After cooling the reaction mixture to room temperature, the crude reaction mixture is dried under reduced pressure. DCM (50 mL) is added and the organic phase is washed with Na_2CO_3 (10 wt%) and water, dried over $MgSO_4$ and evaporated under vacuum. The product is then purified two times by column chromatography on silica gel, eluting with DCM/EtOAc 98:2 – 50:50 gradient (R_f ~ 0.2–0.3) yielding the pure amino ester as a colorless oil (1.30 g, 4.3 mmol, 57%). **^{1}H NMR** (300 MHz, $CDCl_3$): δ 4.10 (t, *J* = 6.7 Hz, 2H), 3.17 (s, 1H), 1.75 (br s, 2H), 1.73-1.51 (m, 2H), 1.43-1.08 (18H), 0.98 (s, 9H), 0.88 (t, *J* = 6.7 Hz, 3H).

Step2: In a flame-dried round-bottom flask under argon atmosphere, benzene-1,3,5-tricarboxylic acid chloride (0.35 g, 1.3 mmol, 1.0 equiv.) is dissolved in dry DCM (50 mL) at room temperature. The amino ester (1.30 g, 4.3 mmol, 3.3 equiv.) is then added in one portion, and the resulting mixture is cooled to 0°C with an ice/water bath. Et_3N (0.6 mL, 4.3 mmol, 3.3 equiv.) is then added dropwise, the reaction is let warm to room temperature and stirred for 48h. Brine is then added to the flask, and the crude mixture is extracted thrice with DCM. The combined organic phases are dried over $MgSO_4$, filtered, and the solvent is evaporated under reduced pressure. The resulting solid is taken up as a slurry in a little DCM, and purified on a short column of silica gel (elution: DCM/EtOAc 6:1) to remove salts and impurities (R_f ~ 0.85-0.9). The product is then purified by column chromatography on silica gel, eluting with DCM/EtOAc 95:5 – 80:20 gradient (R_f ~ 0.2–0.3), yielding pure **BTA *tert*-Leu** (1.20 g, 1.1 mmol, 84%) as a gum-like solid.

^{1}H NMR (300 MHz, acetone-d6): δ 8.40 (s, 3H), 7.85 (d, *J* = 9.0 Hz, 3H), 4.63 (d, *J* = 9.0 Hz, 3H), 4.22–4.10 (m, 6H), 1.73-1.64 (m, 6H), 1.51–1.21 (m, 54H), 1.11 (s, 27H), 0.89 (t, *J* = 6.9 Hz, 9H); **^{13}C{^{1}H} NMR** (75 MHz, acetone-d6): δ 171.8, 167.0, 136.1, 130.2, 65.6, 62.2, 35.2, 32.7, 30.4, 30.3, 30.3, 30.0, 29.4, 27.3, 26.8, 23.4, 14.4; **HRMS:** Calculated for $C_{63}H_{112}N_3O_9$ $[M+H]^+$: 1053.8393, found: 1053.8391. IR (solid) see Figure S.5. *ee*>99%, *de*>99% (page S36).

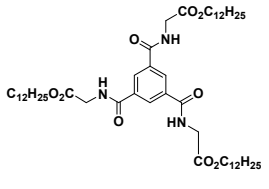

BTA Gly

Tri-N-[dodecyloxycarbonymethyl]benzene-1,3,5-tricarboxamide (BTA Gly)

Step1: In a Dean-Stark apparatus-mounted two-neck flask, Glycine (1.14 g, 15.0 mmol, 1.0 equiv.) is suspended in toluene (0.10 M, 150 mL), and *p*-TsOH.H_2O (3.42 g, 18.0 mmol, 1.2 equiv.) is added at room temperature. Dodecanol (3.35 g, 18.0 mmol, 1.2 equiv.) is then added, and the resulting slurry is stirred at reflux temperature overnight. After cooling the reaction mixture to room temperature, the solvent is evaporated and the crude reaction mixture is dried under reduced pressure to give a solid. This solid is taken up in *ca.* 100 mL of Et_2O, gently heated to 35°C, and let cool to room temperature. The resulting precipitate is quickly filtered under vacuum and washed with cold ether. The white solid is then dried under vacuum to yield the pure ammonium tosylate (5.78 g, 13.9 mmol, 93%). **^{1}H NMR** (300 MHz, DMSO-d6): δ 8.16 (br s, 3H), 7.47 (d, *J* = 7.5 Hz, 2H), 7.11 (d, *J* = 7.7 Hz, 2H), 4.14 (t, *J* = 6.3 Hz, 2H), 3.82 (s, 2H), 2.29 (s, 3H), 1.74-1.53 (m, 2H), 1.49-1.07 (m, 18H), 0.85 (t, *J* = 6.2 Hz, 3H).

Step2: In a flame-dried round-bottom flask under argon atmosphere, benzene-1,3,5-tricarboxylic acid chloride (0.67 g, 2.5 mmol, 1.0 equiv.) is dissolved in dry DCM (100 mL) at room temperature. The ammonium tosylate (3.43 g, 8.3 mmol, 3.3 equiv.) is then added in one portion, and the resulting mixture is cooled to 0°C with an ice/water bath. Et_3N (2.3 mL, 16.5 mmol, 6.6 equiv.) is then added dropwise, the reaction is let warm to room temperature and stirred for 48h. Brine is then added to the flask, and the crude mixture is extracted thrice with DCM. The combined organic phases are dried over $MgSO_4$, filtered, and the solvent is evaporated under reduced pressure. The resulting solid is taken up as a slurry in a little DCM, and purified on a short column of silica gel (elution: DCM/EtOAc 6:1) to remove salts and impurities (R_f ~ 0.85-0.9). The product is then purified by column chromatography on silica gel, eluting with DCM/EtOAc 60:40 – 50:50 gradient (R_f ~ 0.1–0.2), yielding pure **BTA Gly** (1.89 g, 2.1 mmol, 85%) as a crystalline solid.

^{1}H NMR (300 MHz DMSO-d6): δ 9.20 (t, *J* = 5.9 Hz, 3H), 8.51 (s, 3H), 4.09-4.03 (m, 12H), 1.63–1.49 (m, 6H), 1.37–1.14 (m, 54H), 0.85 (t, *J* = 6.9 Hz, 9H); **^{13}C{^{1}H} NMR** (75 MHz, DMSO-d6): δ 169.7, 165.7, 134.3, 128.9, 64.4, 41.4, 31.2, 29.0, 29.0, 28.9, 28.9, 28.7, 28.6, 28.1, 25.3, 22.1, 13.9; **HRMS:** Calculated for $C_{51}H_{88}N_3O_9$ $[M+H]^+$: 886.6515, found: 886.6515. IR (solid) see Figure S.5.

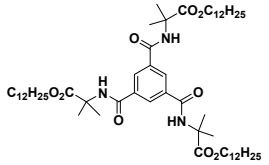

BTA Aib

Tri-N-[(1,1'-dimethyl)dodecyloxycarbonymethyl]benzene-1,3,5-tricarboxamide (BTA Aib)

Step1: In a Dean-Stark apparatus-mounted two-neck flask, 2-aminoisobutyric acid (1.60 g, 15.5 mmol, 1.0 equiv.) is suspended in toluene (0.19 M, 150 mL), and *p*-TsOH.H_2O (4.14 g, 21.8 mmol, 1.4 equiv.) is added at room temperature. Dodecanol (3.19 g, 17.1 mmol, 1.1 equiv.) is then added, and the resulting slurry is stirred at reflux temperature overnight. After cooling the reaction mixture to room temperature, the solvent is evaporated and the crude reaction mixture is dried under reduced pressure to give a solid. This solid is taken up in *ca.* 100 mL of Et_2O, gently heated to 35°C, and let cool to room temperature. The resulting precipitate is quickly filtered under vacuum and washed with cold ether. The white solid is then dried under vacuum to yield the pure ammonium tosylate (6.51 g, 14.6 mmol, 94%). **^{1}H NMR** (300 MHz, DMSO-d6): δ 8.35 (br s, 3H), 7.45 (d, *J* = 7.5 Hz, 2H), 7.12 (d, *J* = 7.7 Hz, 2H), 4.15 (t, *J* = 6.4 Hz, 2H), 2.29 (s, 3H), 1.70-1.53 (m, 8H), 1.45-1.07 (m, 18H), 0.85 (t, *J* = 6.2 Hz, 3H).

Step2: In a flame-dried round-bottom flask under argon atmosphere, benzene-1,3,5-tricarboxylic acid chloride (1.06 g, 4.0 mmol, 1.0 equiv.) is dissolved in dry DCM (100 mL) at room temperature. The ammonium tosylate (6.45 g, 14.4 mmol, 3.6 equiv.) is then added in one portion, and the resulting mixture is cooled to 0°C with an ice/water bath. Et_3N (4.0 mL, 29.5 mmol, 7.4 equiv.) is then added dropwise, the reaction is let warm to room temperature and stirred for 48h. Brine is then added to the flask, and the crude mixture is extracted thrice with DCM. The combined organic phases are dried over $MgSO_4$, filtered, and the solvent is evaporated under reduced pressure. The resulting solid is taken up as a slurry in a little DCM, and purified on a short column of silica gel (elution: DCM/EtOAc 6:1) to remove salts and impurities ($R_f \sim 0.85$-0.9). The product is then purified by column chromatography on silica gel, eluting with DCM/EtOAc 95:5 – 75:25 gradient ($R_f \sim 0.1$–0.2), yielding pure **BTA Aib** (3.41 g, 3.5 mmol, 88%) as a gum-like solid.

^{1}H NMR (300 MHz, acetone-d6): δ 8.37 (s, 3H), 8.24 (s, 3H), 4.09 (t, *J* = 6.5 Hz, 6H), 1.66–1.57 (m, 24H), 1.14–1.18 (m, 54H), 0.88 (t, *J* = 6.9 Hz, 9H); **^{13}C{^{1}H} NMR** (75 MHz, acetone-d6): δ 184.3, 175.7, 145.7, 139.3, 75.2, 67.1, 42.4, 40.0, 39.7, 39.1, 36.4, 35.2, 33.0, 24.1 (some *C*H_2 signals are masked below the solvent peaks); **HRMS:** Calculated for $C_{57}H_{100}N_3O_9$ $[M+H]^+$: 970.7454, found: 970.7453. IR (solid) see Figure S.5.

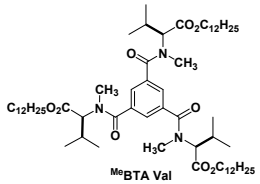

Tri-N-methyl-[(1-isopropyl)dodecyloxycarbonymethyl]benzene-1,3,5-tricarboxamide (^{Me}BTA Val)

^{Me}BTA Val was prepared adapting a published procedure.[10] To suspension of NaH 60% in oil (0.055 g, 1.4 mmol, 6.1 equiv.) in dry THF (2.5 mL) maintained under 20°C by means of a water bath was added a solution of **BTA Val** (0.23 g, 0.22 mmol, 1.0 equiv.) in dry THF/H_2O (2.0 mL : 1 drop, *ca.* 6 µL) dropwise over 20 minutes, keeping the reaction medium under 20°C. The resulting foaming mixture was stirred for 10 minutes before adding neat Me_2SO_4 (120 µL, 1.3 mmol, 5.5 equiv.) dropwise (*caution: very toxic)*. The reaction was then stirred for 1h, maintaining it under 20°C. It was then quenched by slow addition of 30% aq. NH_4OH (1 mL), stirred 1h, and diluted with water (1 mL), then EtOAc (1-2 mL). The resulting mixture was stirred overnight before extraction with AcOEt. The crude product was purified by column chromatography on silica gel, eluting with pentane/AcOEt 8:1 – 4:1 gradient, yielding pure **^{Me}BTA Val** as a pale yellow gum (0.20 g, 0.19 mmol, 86%). NMR analysis was performed in toluene-d8 at 353K a temperature at which the N(CH_3)(R) moieties rotate rapidly on the NMR timescale.

^{1}H NMR (300 MHz, Toluene-d8, 353K): δ 7.70 (s, 3H), 4.61–4.48 (m, 3H), 4.06 (t, *J* = 6.7 Hz, 6H), 2.91 (s, 9H), 2.32-2.14 (m, 3H), 1.57 (t, *J* = 6.7 Hz, 6H), 1.29 (s, 54H), 0.92–0.84 (m, 27H); **^{13}C{^{1}H} NMR** (50 MHz, Toluene-d8, 353K) δ 170.7, 170.6, 138.3, 137.7, 65.3, 32.5, 30.2, 30.1, 29.9, 29.7, 29.2, 28.3, 26.5, 23.1, 14.2. **HRMS:** Calculated for $C_{63}H_{112}N_3O_9$ $[M+H]^+$: 1054.8393, found: 1054.8381. IR (solid) see Figure S.5.

Determination of the optical purity of BTA (*R*)-Cha by chiral HPLC

Method description: column = Chiralpak AZ-H, heptane/ethanol 90/10, flow = 1 mL/min, detection at 254 nm.

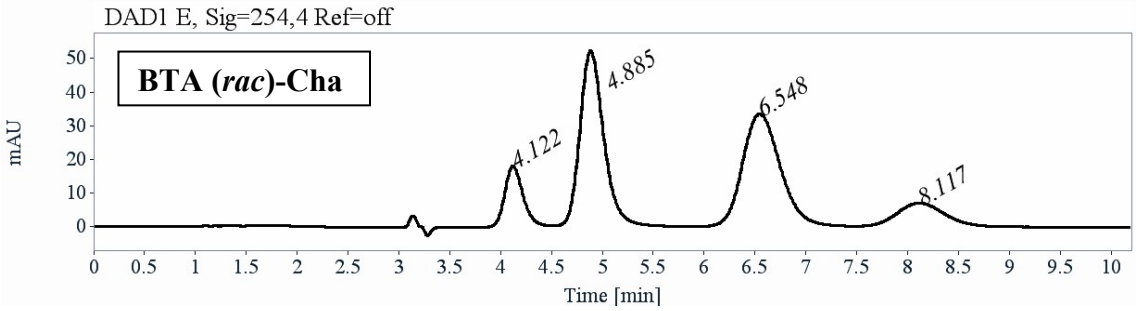

RT [min]	Area%
4.12	10.51
4.89	39.53
6.55	39.58
8.12	10.37

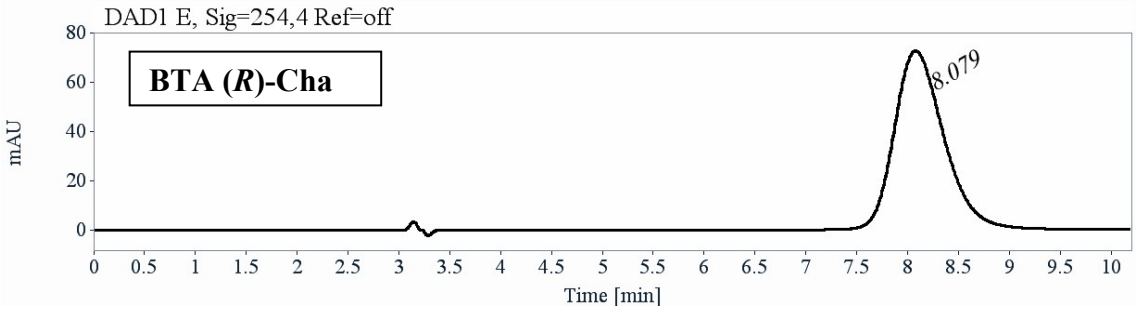

RT [min]	Area%
8.08	100.00

Determination of the optical purity of BTA *tert*-Leu by chiral HPLC

Method description: column = (*S*,*S*)-Whelk-O1, heptane/ethanol 90/10, flow = 1 mL/min, detection at 220 nm.

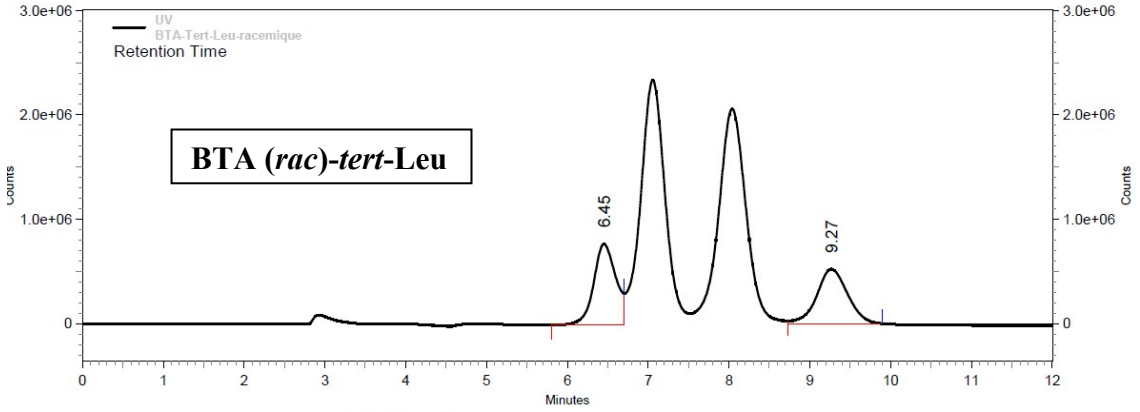

UV Results

Retention Time	Area	Area %
6.45	14819908	11.66
7.06	49092815	38.63
8.04	49273365	38.77
9.27	13890629	10.93

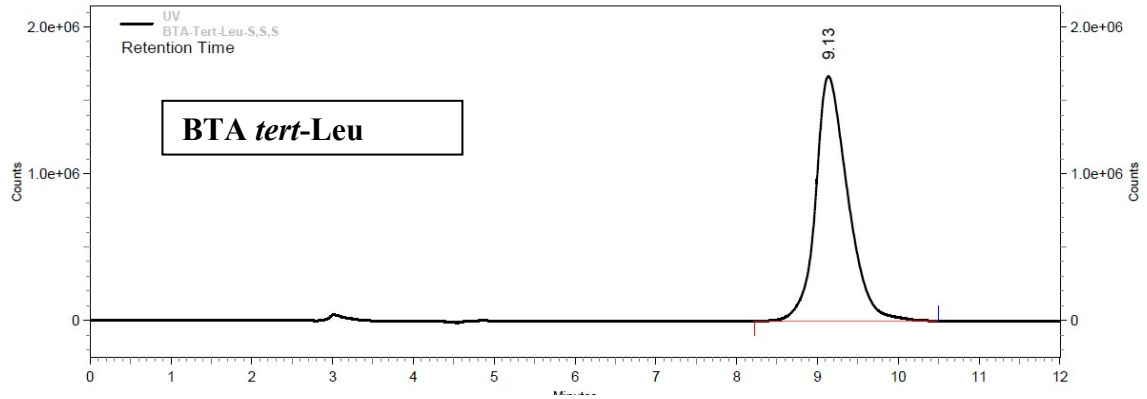

UV Results

Retention Time	Area	Area %
9.13	46179097	100.00

BTA (*R*)-Cha

^{1}H (acetone-d6):

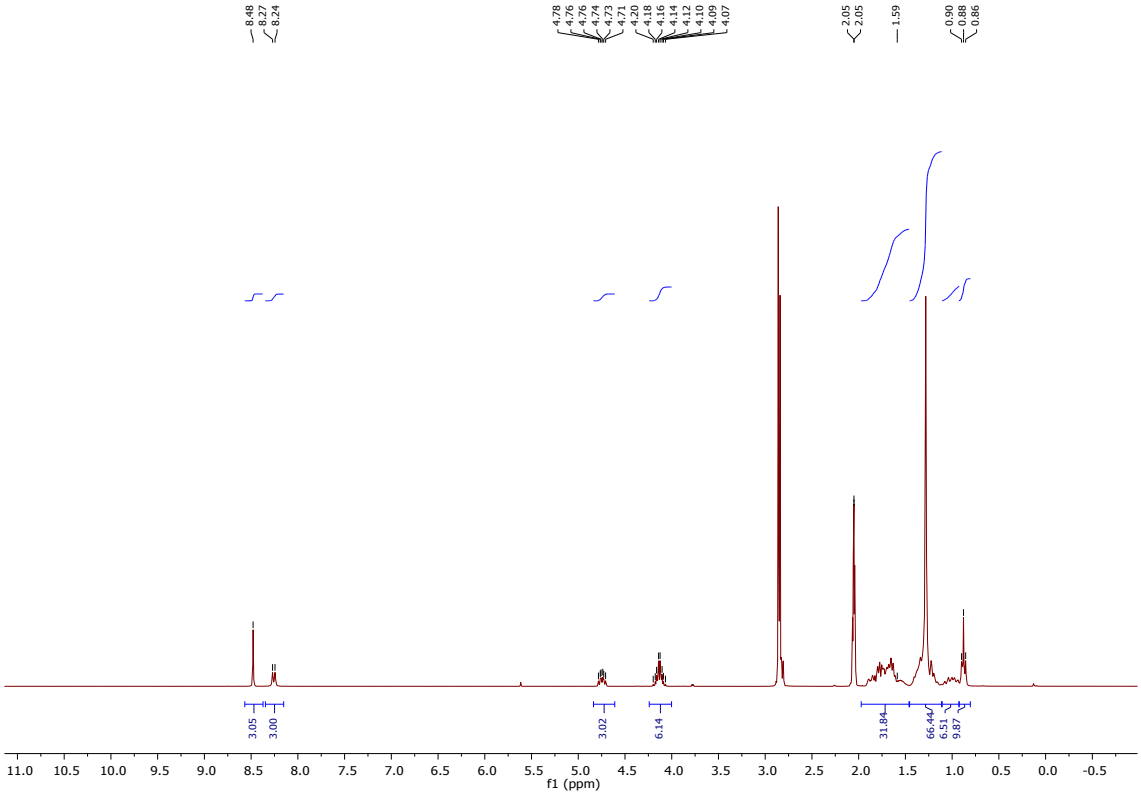

^{13}C{^{1}H} (acetone-d6):

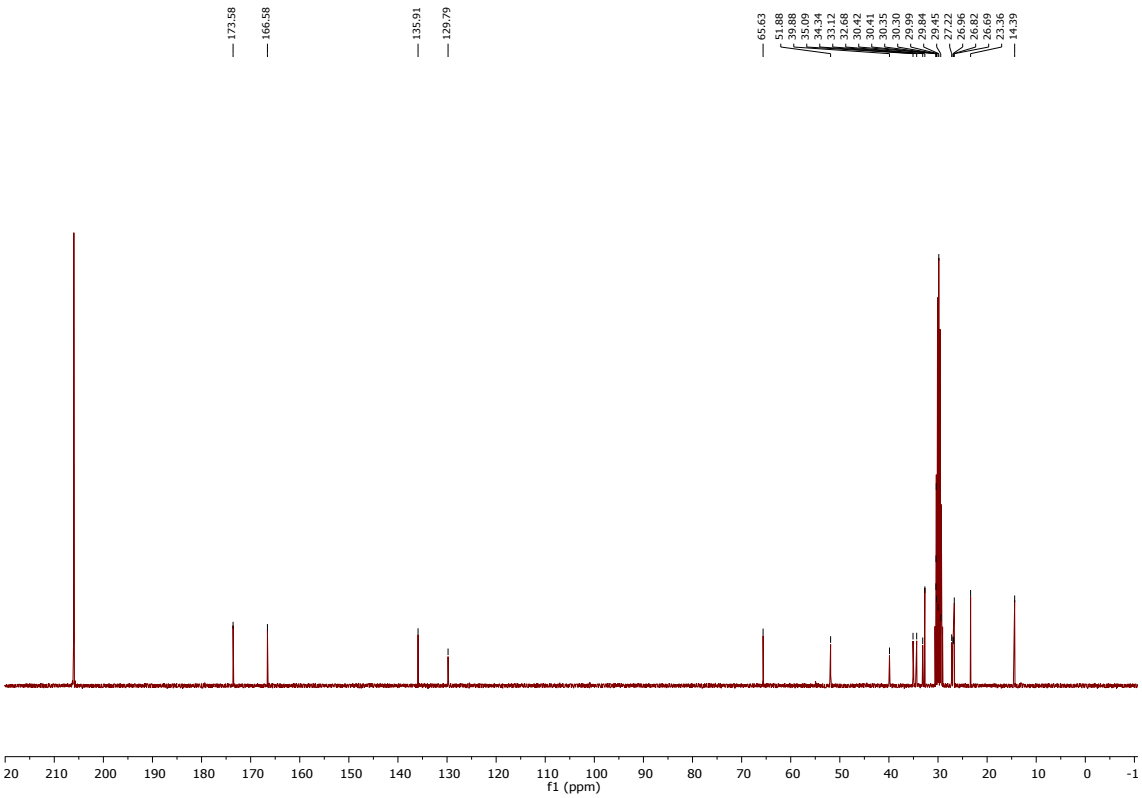

BTA *tert*-Leu

^{1}H (acetone-d6):

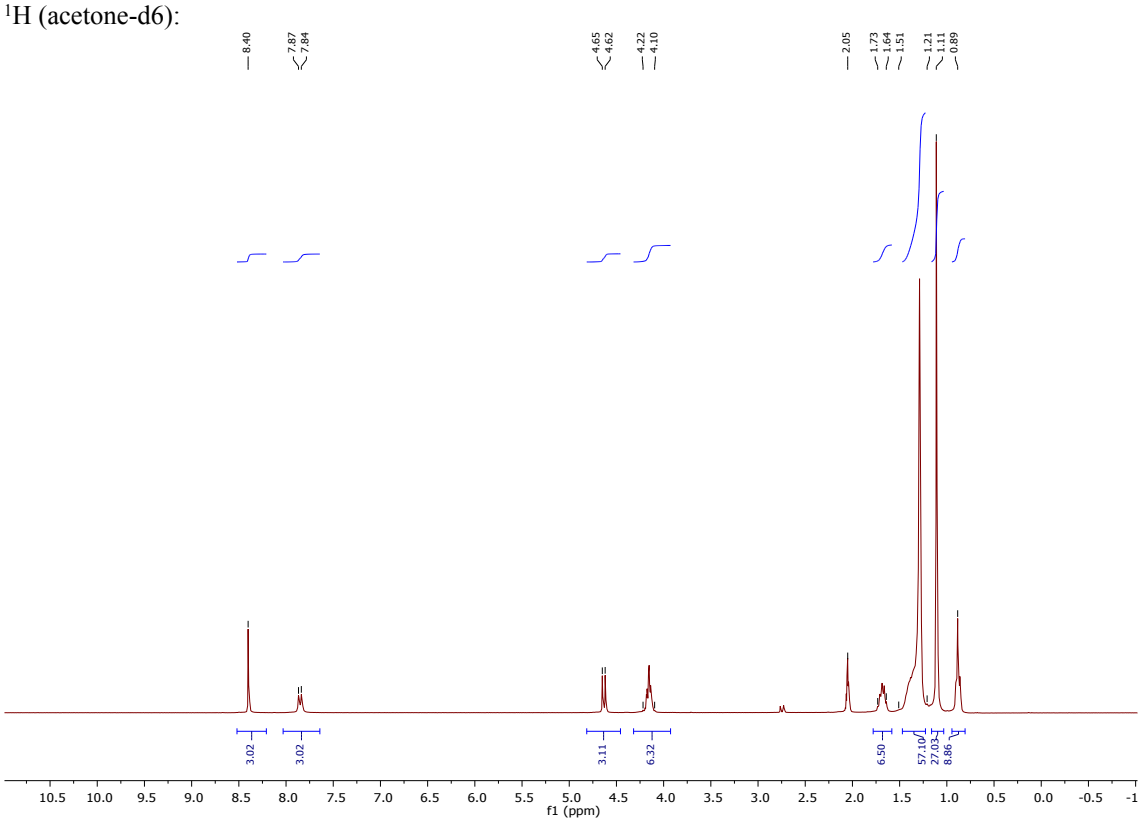

$^{13}C\{^{1}H\}$ (acetone-d6):

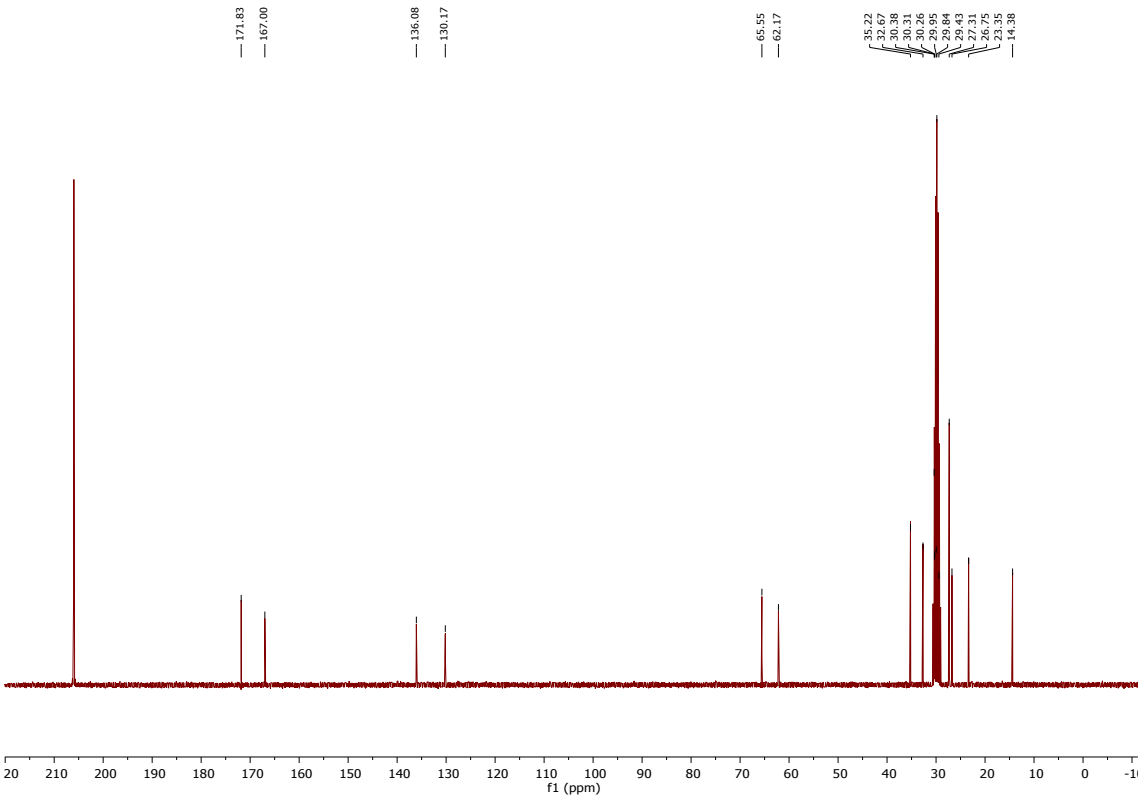

BTA Gly

^{1}H (DMSO-d6):

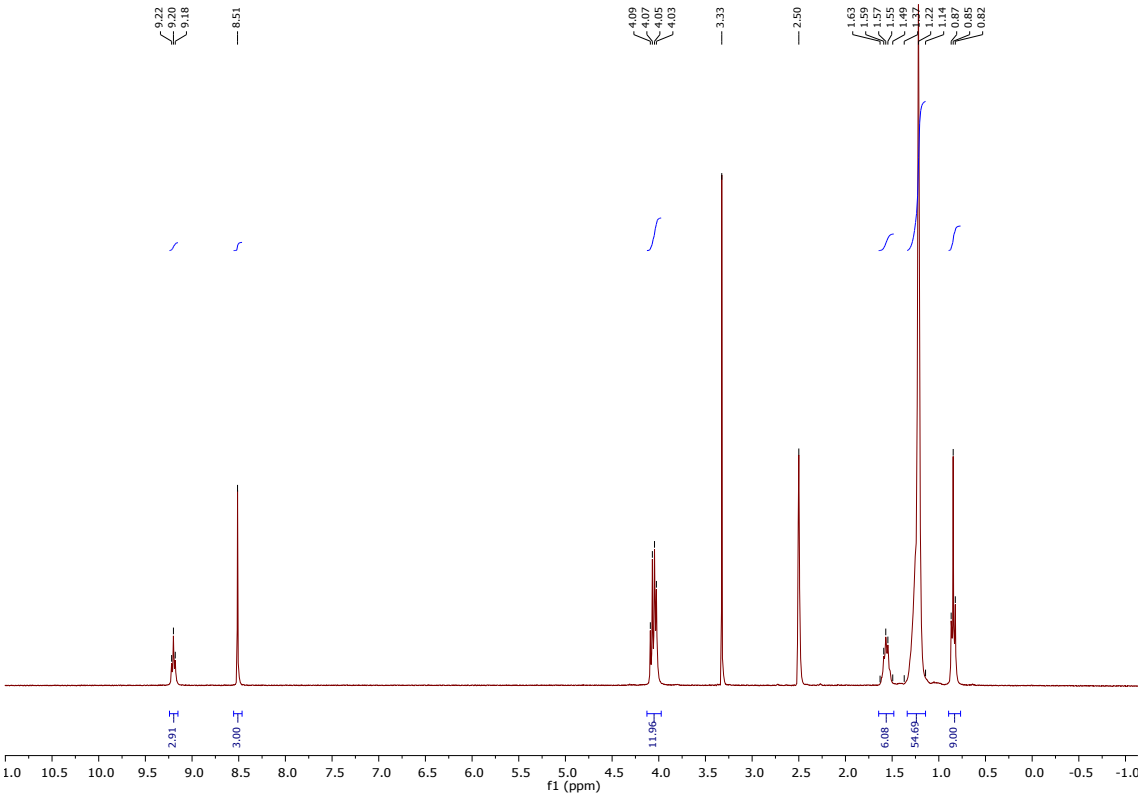

$^{13}C\{^{1}H\}$ (DMSO-d6):

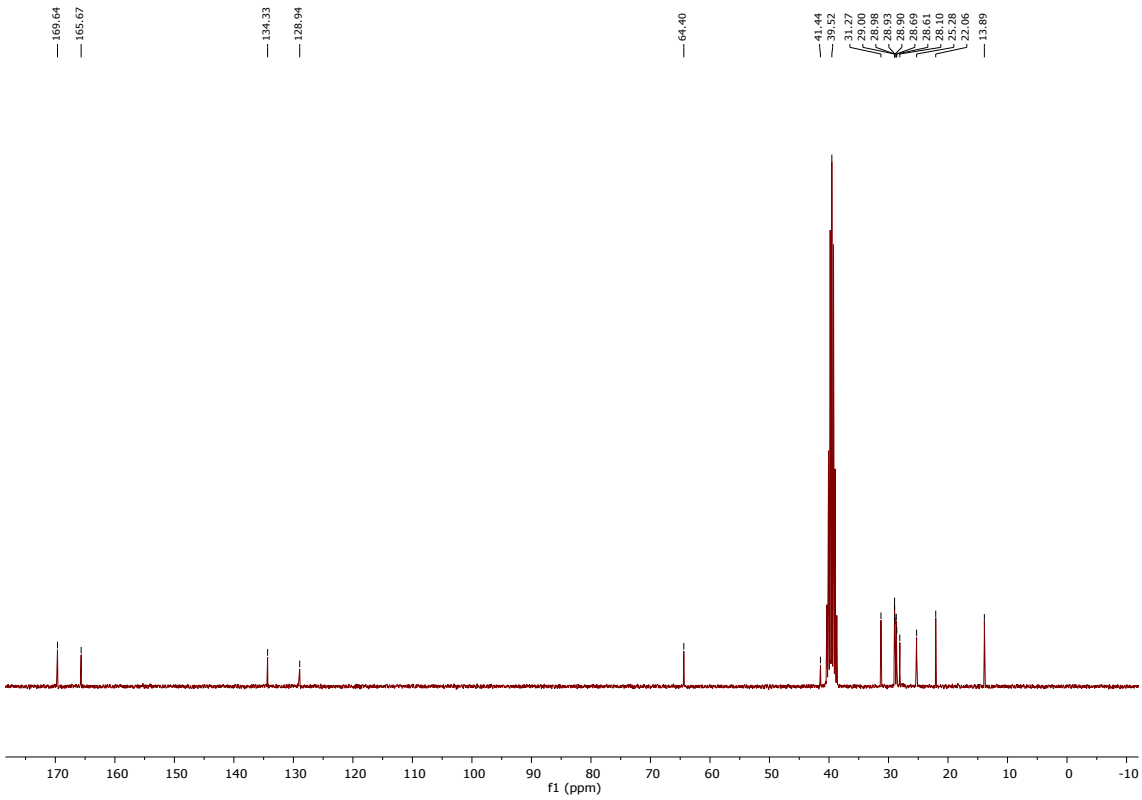

BTA Aib

^{1}H (acetone-d6):

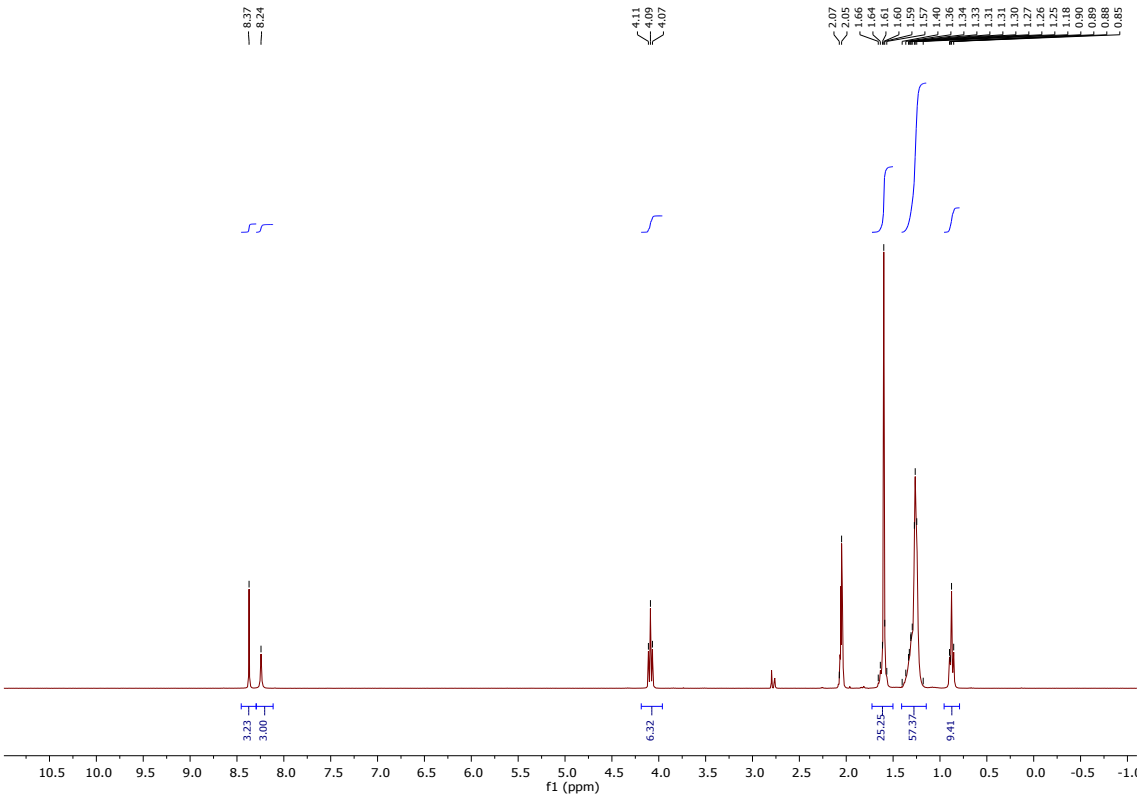

$^{13}C\{^{1}H\}$ (acetone-d6):

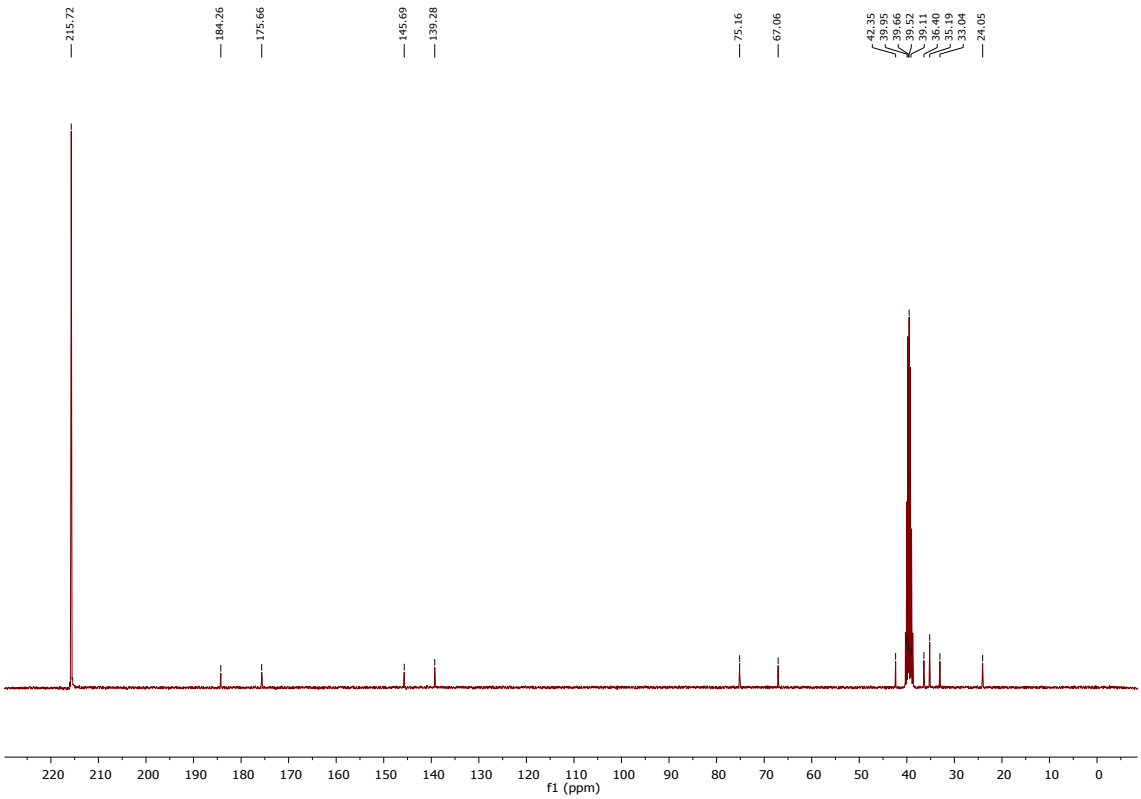

^{Me}BTA Val

^{1}H (toluene-d8, 353K):

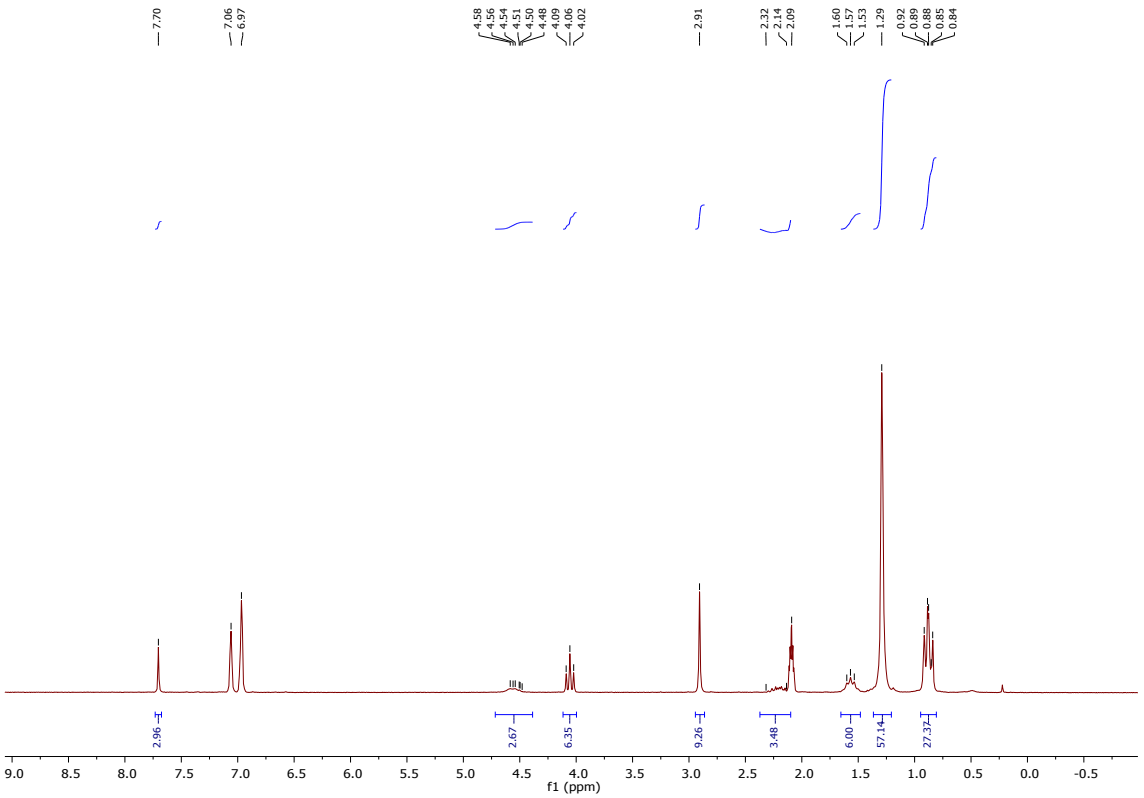

^{13}C{^{1}H} (toluene-d8, 353K):